Neuroimage: Reports 5 (2025) 100271

Contents lists available at ScienceDirect

Neuroimage: Reports

journal homepage: www.sciencedirect.com/journal/neuroimage-reports

Headache-specific hyperexcitation sensitises and habituates on different time scales: An event related potential study of pattern-glare

Cihan Dogan [d], Claire E. Miller [b], Tom Jefferis [d], Margarita Saranti [b], Austyn J. Tempesta [b], Andrew J. Schofield [c], Ramaswamy Palaniappan [a], Howard Bowman [b,d,e,*]

[a] School of Computing, University of Kent, Canterbury, UK
[b] School of Psychology, College of Life and Environmental Sciences, University of Birmingham, Edgbaston, Birmingham, UK
[c] School of Psychology, College of Health and Life Sciences, Aston University, Birmingham, UK
[d] School of Computer Science, University of Birmingham, Edgbaston, Birmingham, UK
[e] Functional Imaging Lab, University College London, [honorary], UK

ARTICLE INFO

Keywords:
EEG
Computational and Cognitive Neuroscience
Headache and Pain
FieldTrip
MATLAB

ABSTRACT

Cortical hyperexcitability is a key pathophysiological feature in several neurological disorders, including migraine, epilepsy, tinnitus, and Alzheimer's disease. We examined the temporal characteristics of Event Related Potentials (ERPs) in a healthy population using the Pattern Glare Test, a diagnostic tool used to assess patients with sensitivity to cortical hyperexcitability. In pre-experiment questionnaires, participants reported their susceptibility to a range of symptoms. A factor analysis over these responses identified three variables, with the one we investigate in this paper loading strongly on headache symptoms, e.g. headache frequency. We investigated two timeframes: habituation over the course of the entire experiment and sensitization over the course of a sequence of stimulus presentations. We found evidence of hyperexcitability at electrodes over visual cortex, for the aggravating stimulus (grating of ~3 cycles/deg). Participants higher on the headache factor exhibited a higher degree of habituation and sensitization, with evidence that the level of sensitization habituated through the course of the experiment. These findings suggest that the same experimental paradigm and analysis should be performed on a clinically diagnosed population.

1. Introduction

Some visual stimuli cause mild discomfort for most observers and considerable discomfort for a minority of sensitive individuals; such stimuli are called pattern glare stimuli (Nulty et al., 1987; Wilkins et al., 1984). The archetypal pattern-glare stimuli consist of striped patterns with a spatial frequency of close to three cycles per degree (Wilkins and Evans, 2001). Stimuli of this kind have been implicated in visually-induced migraine and, even, epilepsy (Wilkins et al., 1984; Adjamian et al., 2004). Accordingly, there is considerable interest in understanding the brain responses to pattern-glare stimuli, since this could indicate the neurological processes that underlie the brain's susceptibility to headache, migraine, and epilepsy. In this respect, it is believed that pattern-glare stimuli could induce a hyper-excitation of central neuronal networks in the brain, a condition that has been implicated in headache and migraine (Welch, D'Andrea, Tepley, Barkley and Ramadan, 1990).

In a classic MEG study, Adjaman et al. (2004) showed that striped patterns at the pattern-glare spatial frequency (~3 cycles/deg), induced a heightened brain response in the form of increased power at gamma (temporal) frequencies. This gamma response is likely an electrophysiological correlate of hyper-excitation in the frequency domain. More recently, in the time-domain, Fong et al. (2020) found differences between migraine sufferers and controls at around 200- and 400-ms post-stimulus onset. Their migraine group showed greater negativity at 200ms for high-frequency gratings (13 c/deg). Indeed, their main findings were on high-frequency gratings, while in contrast, the findings we report occur with aggravating, medium-frequency gratings (3 c/deg).

In addition, Tempesta et al. (2021) presented time-domain findings suggesting that the absence of an N1 (occurring at a time-period between 150 and 200ms post stimulus onset in averaged ERPs) marks the brain's response to pattern-glare stimuli. Additionally, susceptibility to headache predicted the extent of N1 absence such that participants with

* Corresponding author. School of Psychology, College of Life and Environmental Sciences, University of Birmingham, Edgbaston, Birmingham, UK.
E-mail address: h.bowman@bham.ac.uk (H. Bowman).

https://doi.org/10.1016/j.ynirp.2025.100271
Received 8 August 2024; Received in revised form 3 June 2025; Accepted 6 June 2025
Available online 24 June 2025

increased headache propensity exhibited smaller N1s and thus a more positive-going response. This headache-by-brain-response relationship was observed for repetitions of the pattern-glare stimuli, but not for its first presentation in a sequence of between 6 and 9 repeats (interestingly, Fong et al. (2020)'s findings were on the first presentation, perhaps explaining why their findings are different to those we report here, which are on repetitions). This suggests that there may be an habituation component, or failure thereof, to this headache-N1 effect. However, Tempesta et al. (2021) did not directly determine whether their effect changed across repetitions, e.g. from repetition 2 to repetition 3, 3 to 4 and so on, which would be the definitive test of change through time, whether an increase (sensitization), or a decrease (habituation). An objective of this paper is to make such a more detailed assessment of the temporal effects (sensitization/habituation) associated with pattern-glare stimuli across multiple repetitions – which we achieve via a reanalysis of the data presented in Tempesta et al. (2021).

Habituation (or failure thereof) is a key phenomenon in the study of headache and migraine (and epilepsy), with many studies showing dysfunctional habituation for these conditions (Brazzo et al., 2011; Coppola et al., 2009).Thus, understanding how the brain habituates or sensitises to repeating pattern-glare stimuli is of great interest. For example, if one fully understood how hyper-excitability habituates in the brain, one might be able to use that information to develop therapies, which seek to return the brain to an un-hyper-excited (i.e. habituated) state.

We consider two different patterns of change through time: habituation and sensitization. Both reflect an exponential change through time, with the first matching a brain response that reduces through time; the second one that increases. (The choice of exponential change through time is justified in the Methods.) A key question is the temporal granularity at which any sensitization or habituation effect operates. For example, it could occur at relatively fine temporal granularity, such as tens of seconds. Alternatively, it may only be observable across minutes or tens of minutes. Fortunately, Tempesta et al. (2021) presented multiple repeats of each stimulus within each trial with onsets (individual occurrences of the stimulus appearing on screen) about 4 s apart and also divided their experiment into three partitions/blocks, each about 12 min long thus allowing us to answer our key questions about the granularity of habituation/sensitization.

We also consider the effects of the state and trait measures introduced by (Tempesta et al., 2021). They conducted a factor analysis on state (discomfort ratings during the experiment) and trait (questionnaire) variables, producing three factors, which were (in order of factor loading): visual stress (largely trait; sensitivity to visual patterns - particularly stripes), headache (largely trait; susceptibility to headaches) and discomfort (largely state; feelings of heightened discomfort when viewing 3 c/deg stimuli during an experiment involving repeated presentation of striped stimuli). Visual stress refers to discomfort or perceptual distortions triggered by high-contrast repetitive patterns, particularly around 3 cycles per degree, and is linked to cortical hyperexcitability and conditions such as migraine and photosensitive epilepsy (Wilkins et al., 1984). These factor scores reflect the susceptibility of each participant to relevant health conditions and symptoms.

This paper focuses on effects associated with the Headache factor: these being our strongest effects.[1] A companion paper (Dogan et al., 2025) focuses on the remaining effects, associated with the visual stress and discomfort factors on early transients. Our statistical inference is formulated over continuous regressors. Fig. 1 illustrates how three of these are constructed. These are used by FieldTrip in Mass Univariate Analyses (MUA). For each question of interest, a design matrix is constructed, representing the regressor predictors. For example, Fig. 1 (a) addresses the question: "Does the headache factor predict EEG activity (relative to baseline). Informally, when a participant is high on the headache factor, is their EEG activity also high?" This is tested statistically by fitting a regression model, where we are using headache scores to predict EEG data. (Actually, we predict their pattern-glare index, see sub-section "Hyper-excitation" and section 2, "Methods", a derived measure reflecting hyper-excitation of the EEG). This is performed separately across all electrodes and time points. Full details of this procedure are described in the Methods section.

Illustrations of the two-way interactions are shown in Fig. 1(b), with the response to the headache factor changing across three time-points. The first interaction plot (left panel of 1bi) models headache-by-habituation. This reflects the intuition that (i) the brain's response will vary considerably with headache-proneness at the first time point (red line), with those high on the factor showing larger responses, as implied by hyper-excitation, (ii) variability then reduces through time (green line), until (iii) all hyper-excitation has dissipated and all participants exhibit the same (low) response at the final time-point (blue line). Headache-by-Sensitization (right panel of 1bi) represents the alternative hypothesis that hyper-excitation emerges through the three time-points, leading to high variability in brain response at the final time-point, with those high on the headache factor exhibiting large (hyper-excited) responses. Fig. 1bii outlines how these regressors are integrated into the regression equation that Fieldtrip fits.

To answer our main question, we test these factor-by-time interactions at the two time-granularities offered by the Tempesta et al. (2021) data: *fine*, i.e., repetitions within a single trial (with about 4 s between onsets) and *coarse*, i.e., partitions of the entire experiment (with each partition lasting 10–12 min). We call the fine granularity *onsets* and the coarse granularity *partitions*.

1.1. Hyper-excitation

Our experiments will use three stimuli: gratings at 3 c/deg, the aggravating pattern-glare stimulus, and two control stimuli at spatial frequencies on either side of 3 c/deg. According to their spatial frequency, we will call the aggravating stimulus the Medium, and the two control stimuli, Thin and Thick. This is consistent with the, previously discussed, stimuli used in (Fong et al., 2020) and (Tempesta et al., 2021).

We operationalize hyper-excitation as the electrical response of the brain being "larger" for the Medium stimulus than for the Thin and Thick, strictly than for the mean of Thin and Thick. Although, "larger" here actually means more extreme from zero, whether in a positive or negative direction. This is because the polarity of an EEG signal reflects the orientation of the electrical dipole to the recording electrode, meaning that a response of +X micro-volts is in no sense a bigger electrical response than a response of -X micro-volts. We call the Medium minus the mean of Thick and Thin the *pattern-glare index*. If the amplitude of Medium would be equal to the amplitude of the mean of Thick and Thin, then EEG amplitudes would just reflect spatial frequency, and the pattern-glare index would be zero. Any divergence of the pattern-glare index from zero, suggests that the brain is responding in a different way to spatial frequency, raising the possibility of hyper-excitation.

1.2. Hypotheses

To be specific, we have the following hypotheses.

1) Participants susceptible to headaches will exhibit sensitization at short timescales, i.e. hyper-excitation will increase across repeating presentations, over a relatively fine temporal period, of a few seconds.

[1] We also present analyses where we orthogonalize the headache factor regressors with regard to the other factor regressors in Appendix A5. This reflects the fact that they were obtained from the same factor analysis, and we want to guard against benefiting multiple times from the same variability in the data.

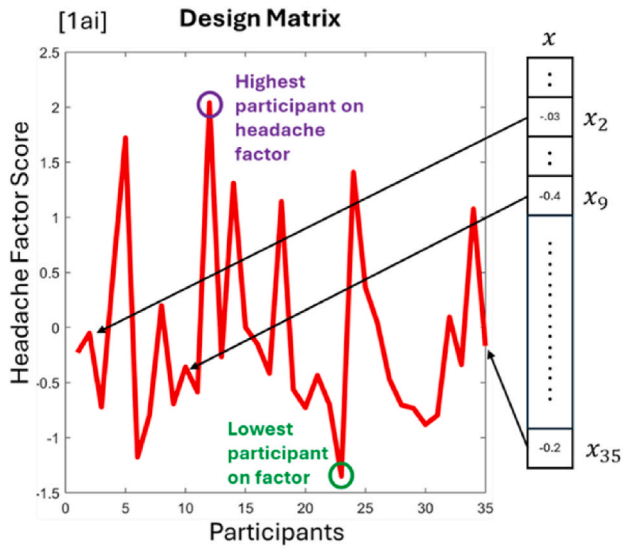

[1aii]

Regression Equation:

$$y_i = \beta . x_i + C + e_i$$

y_i: dependent variable of 35 x 1 (35 rows, which i ranges over): electrical brain response (EEG), with a value for every participant (i) run in the analysis.

x_i: independent variable, a single regressor column vector of 35 x 1, of a participant's Headache score.

β: coefficient inferred from fitting regression model.

C: model intercept

e_i: residual error

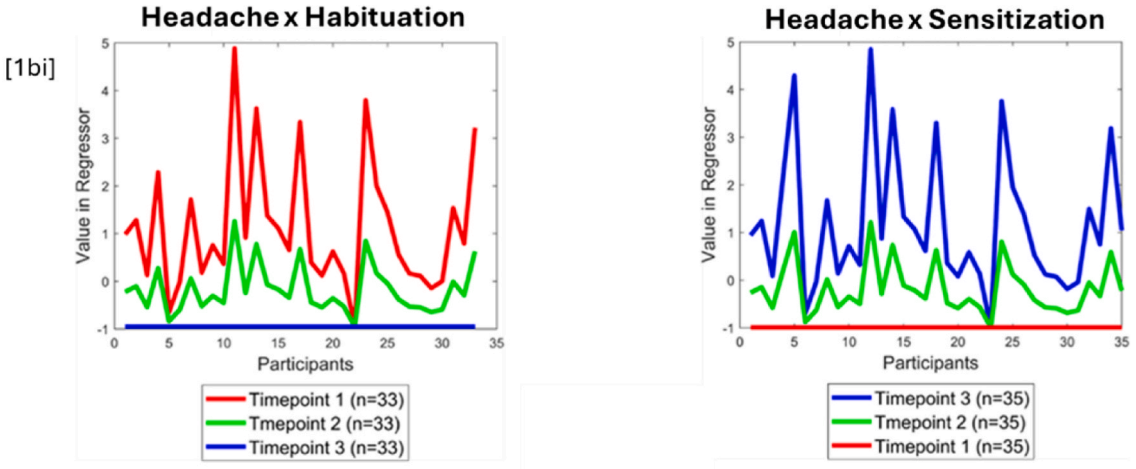

[1bii] **Regression Equation:** $y_i = \beta . x_i + C + e_i$

n: number of participants run in analysis.

y_i: dependent variable, column vector of 3.n rows (which i ranges over): electrical brain response (EEG), with a value for every participant (i) run in analysis, for each of (three) time points.

x_i: independent variable, a single regressor column vector of 3.n rows; effect "searched" for in data, with a value for every participant (i) run in analysis, for each of (three) time points; constructed from one of panels in [1bi], with three horizontal lines (red, green and blue) turned and concatenated into a single (vertical) column vector.

β: regression coefficient inferred; C: model intercept; e_i: residual error

Throughout figure, what we refer to as "electrical brain response" (i.e. y_i), is in fact, a derived EEG measure, the pattern-glare index, see below.

Fig. 1. Illustration of regressors: [1a] Example of Headache factor: [1ai] Headache factor scores, one for each participant, and how those scores become a column vector regressor. [1aii] Form of regression model, containing column vector regressor. [1b] Example of two two-way interaction regressors: [1bi] shows the Headache x Habituation (left) and Headache x Sensitization (right) interaction regressors. For the habituation regressor, a declining trend is observed through the time-points, representing an habituation effect through time. (For the sensitization regressor, an increasing trend is observed through the time-points.) [1bii] is the regression equation and explanation for the simple linear regression used in the FieldTrip toolbox. Since FieldTrip can only perform family-wise error correction with a single continuous regressor (along with the intercept), we have had to build single regressors for all effects. Please refer to the manuscript online for colour versions of the figure.

2) For those same participants susceptible to headaches, we also believe that they will exhibit a change in hyper-excitation over the coarser time resolution, of the entire experiment. However, the direction of this effect was less clear before collecting the data. We may also see sensitization through the course of the entire experiment, because we are continuing to drive the system with an aggravating stimulus. However, we may observe habituation across this longer time-period because even our participants who are sensitive to the Medium stimulus, have not been clinically diagnosed with migraine, headache or epilepsy. Accordingly, their brains may successfully habituate to the Medium stimulus, with sufficient presentations.

3) Finally, it is also possible that we will observe an interaction between the two different time granularities, which might, for example, show that sensitization to repeated presentation of the Medium stimulus only obtains at the start of the experiment, when those susceptible to headaches are first subjected to the aggravating stimulus. With this effect waning through the course of the experiment, i.e. their brains habituating.

To pre-empt our findings, we do indeed identify evidence for fine time-granularity (across onsets) sensitization and coarse time-granularity (across partitions) habituation in response to pattern-glare stimuli. Additionally, these effects are modulated by headache, being most clearly evident in those high on the headache factor. This indeed suggests that, in our (non-clinical) population, short time-frame repetition induces hyper-excitation for those susceptible to having headaches, but their brains are able to respond to this hyper-excitation and habituate across the course of the experiment.

2. Methods

Our methods are, by necessity, identical to those reported by Tempesta et al. (2021) whose data we reanalyse. However, for completeness, we present a comprehensive summary here.

2.1. Dataset/participants

Forty participants were initially recruited at the University of Birmingham, all gave informed consent and were compensated with £24 for participating. They had no neurological, psychiatric, or psychological conditions, as well as no history of unconsciousness, convulsions, or epilepsy. Two of the participants were excluded prior to pre-processing, as one left the experiment before completion and the other because of an equipment malfunction. Additionally, during the pre-processing phase, we ensure that at least 20 % of useable trials exist per condition, consistent with guidelines from (Luck, 2014). This means that different conditions will have different numbers of participants (see Table 1). For example, participant A may have at least 20 % of useable trials in each group of onsets (2,3; 4,5; 6,7) and therefore would be included in the Sensitization analyses. However, this participant may not have 20 % of useable trials in the first partition of the experiment and as a result would be excluded in any Habituation analysis (see Table 1). The study was ethically approved by the Science Technology Engineering and Maths Ethics Committee at the University of Birmingham.

2.2. Stimuli/equipment

The stimuli were created with the Psychophysics Toolbox in MATLAB (Brainard, 1997; Kleiner et al., 2007; Pelli, 1997) and were based on those from the Pattern-Glare Test (Wilkins and Evans, 2001). The stimuli were horizontal square-wave gratings at 3 different spatial frequencies (0.37, 3, and 12 c/deg: described as *thick*, *medium*, and *thin* respectively; see Fig. 2), and they were displayed at 75 % contrast in a circular window, with a diameter of 15.2 deg, at a viewing distance of 86 cm. The stimuli were displayed on a 60 Hz Samsung 932BF LCD monitor (Samsung Electronics, Suwon, South Korea) with pixel pitch 0.02 deg/pixel. Each cycle of the 12c/deg grating occupied 4 screen pixels; 3 c/deg, 16 pixels; and 0.37 c/deg, 130 pixels respectively, such that our stimuli were represented without spatial aliasing. Stimuli were calibrated against the monitor's gamma non-linearity such that the luminance of the grey background matched the mean luminance of the gratings. In the behavioural PGI test, pattern 1 (thick) is a control for response bias and is useful in detecting 'which patients may be highly suggestible and may respond yes to any question about visual perception distortions' (Evans BJ, 2008). In our context, pattern 1 (thick) also contributes to our control of individual differences in brain responses; see end of paragraph. Pattern 2 (medium) is the only clinically relevant stimulus falling between spatial frequencies 1–4, which are known to elicit migraines, headache and epileptic seizures (Braitwaite et al., 2013; Wilkins A. J., 2015). Pattern 3 (thin) is a control for poor convergence and accommodation. Those with poor convergence and/or accommodation will see distortions in this stimulus reflecting optical rather than neurological factors (Conlon E. , Lovegrove, Barker and Chekaluk, 2001). A further reason for including pattern 1 (thick) and pattern 3 (thin) is to accommodate individual differences in the brain response to gratings. That is, some participants may have a larger evoked response to all gratings. By focusing our analysis on how different the response to pattern 2 (medium) is to the response to the average of pattern 1 (thick) and pattern 3 (thin) (see definition of Pattern Glare Index (PGI) in subsection "Design Matrices and Mass-univariate Analysis"), we are able to subtract out these individual differences.

The EEG recordings employed a 128-channel BioSemi EEG system and were made in a dark, quiet room.

Table 1
A breakdown of age, gender and number of participants by condition. In all conditions, apart from the Mean/Intercept, these conditions are crossed with the headache factor.

Experiment Type	Age (mean ± standard deviation)	Gender	Total Participants
Mean/Intercept	22.5 ± 2.9	14 male, 21 female	35
Habituation through Onsets	22.42 ± 2.2	14 male, 21 female	35
Habituation through Partitions	21.96 ± 2.3	12 male, 22 female	34
Sensitization through Partitions	21.96 ± 2.3	12 male, 22 female	34
Sensitization through Onsets	22.42 ± 2.2	14 male, 21 female	35
Three-way interaction	21.32 ± 2.1	12 male, 20 female	32

2.3. Questionnaires

For the assessment of headache symptoms, we selected relevant questions from a more general Headache and General Health questionnaire. Thus, we did not use the headache criteria specified by the International Headache Society (IHS, 2018) to diagnose migraine. These are criteria for clinical diagnosis and do not provide scale measures of headache proneness. However, the criteria rely heavily on headache intensity, duration, and frequency, and the presence of aura (covering a wide variety of sensory/motor disturbances), all of which were assessed by our questions. For further details of these questions, see Supplementary Material/Appendix A2 (titled, "Headache Questions").

Questionnaires were also used to assess participants' tendency to suffer visual stress and cortical hyperexcitability. The Visual Discomfort Scale (VDS) (Conlon et al., 1999) is a 23-item questionnaire measuring susceptibility to visual discomfort, with higher scores correlating with headache severity, visual distortions, and cognitive performance deficits. Similarly, the Cortical Hyperexcitability Index (CHi) (Braithwaite et al., 2015) is a 27-item questionnaire assessing an individual's general tendency to experience episodes of cortical hyperexcitability, based on past experiences.

2.4. Procedure

Following electrode application, the experiment began with a 5-min resting period. The main experiment consisted of 3 blocks (partitions) each with 6 trials per stimulus type (thin, medium, thick), totalling 18 trials per stimulus. The trial sequence is shown in Fig. 3. Each trial began with a fixation cross displayed for 4 s, followed by 7–9 onsets of one kind of stimulus for 3 s each, and ending with a fixation interval lasting between 1 and 1.4 s (varied at random). The stimulus was shown on the

Fig. 2. The three types of stimuli (thick, medium, thin) used in the Pattern Glare Test. Note that these images are representative of the stimuli used in the experiment but are rendered here to aid visibility.

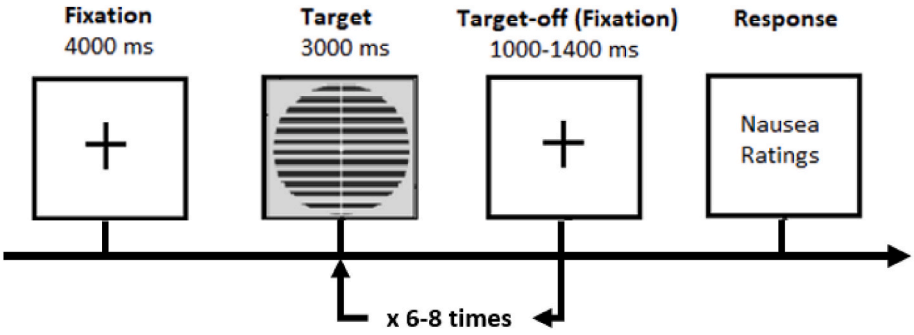

Fig. 3. Schematic representation of one trial. This whole sequence was repeated 6 times per stimulus type to complete one block of the experiment.

screen for the complete 3 s interval, without flicker. After each trial, the participants were asked to rate how comfortable they felt on a scale of 1 (= no discomfort) to 5 (= extreme discomfort), and the number of onsets they observed so that their attentiveness could be estimated. Following each block, the 3 stimuli were presented to the participants consecutively, and they were asked to report the extent to which they had experienced any of the possible pattern-glare symptoms for each one (Wilkins and Evans, 2001). After each block and following the conclusion of the experiment, the participants had a 5-min break during which they were asked to relax and close their eyes. The stimulus order and onsets per trial were counterbalanced between participants.

2.5. Factor analysis

Our analysis of the factors followed Tempesta et al.'s analysis and included all 39 participants who completed the study, as factor analysis benefits from larger datasets. Data for headache frequency, intensity and duration and the experience of sensory aura (see Supplementary Material/Appendix A2, titled, "Headache Questions") were extracted.

The seven measures (DI, Chi, VDS, Aura, Headache -frequency, -intensity and -duration) were standardised before factor analysis. A Scree plot presented factors which, following Varimax rotation, were identified (in eigenvalue order) as visual stress (predominantly a combination of CHi, VDS and aura), headache (frequency, intensity, and duration) and discomfort (DI). Initial factor scores were computed using the regression method from coefficients shown in Supplementary Material/Appendix A3 (titled "Factor Analysis"), where we also describe the factor analysis in more detail. Further analysis investigated the reliability of applying dimensionality reduction techniques (PCA; Factor Analysis; Averaging) to our behavioural data. We concluded that, Factor Analysis is a reliable decomposition method in the context of our data. Please refer to Supplementary Material/Appendix A4 (titled "Justification of factor analysis decomposition").

The factor structure described above is unsurprising given the variables included, but the analysis was also intended to provide orthogonal factors. When we further reduced the number of participants, as a result of artefact rejection, our factors were no longer fully orthogonal, although this loss of orthogonality was small. Nonetheless, departing from (Tempesta et al., 2021), we orthogonalized headache and discomfort with respect to visual stress (the strongest factor) on this smaller number of participants. This was done using the Gram–Schmidt algorithm (Arfken, 1985).

2.6. EEG pre-processing

Our EEG processing diverges from that of (Tempesta et al., 2021), although in common with them we down sampled the EEG data from a sampling rate of 2048 to 512 Hz using the Biosemi toolbox. Eye-blink artefacts were removed using independent component analysis (ICA), with ICA components associated with eye blinks removed and the dataset reconstructed.

The FieldTrip toolbox (Oostenveld et al., 2011); version 20210807, was then used for the following pre-processing and analysis. EEGs were band-pass filtered with a FIR filter using a range of 0.1–30 Hz using a Hanning window. Data for each onset were epoched between −200 and 1200ms relative to stimulus onset, referenced to the average of all electrodes and baseline corrected based on the 200ms period prior to stimulus onset. Thresholding was then applied with a 100 μV threshold in both the positive and negative directions, thus removing any large artefacts present in the data. Participants were rejected if after thresholding, less than 20 % of the original trial count remained for any one of the three conditions (Thick, Medium, and Thin), or experiment types (Mean/Intercept, Habituation and Sensitization).

The stimuli were equally probable at the first onset; as a result, onset 1 was not considered in the analysis because it could contain response information reflecting surprise. In contrast, the stimuli presented from onset 2 onwards (within each trial) were completely predictable.

As well as the Factors dimension (which, as previously discussed, has three levels: Visual Stress, Headache and Discomfort), we had a dimension reflecting change through time. For this dimension, we

considered two different patterns of change through time: *habituation* (a reducing brain response through time) and *sensitization* (an increasing brain response through time). These two different patterns of change through time, were applied to two different time granularities (which give the dependent variable for our regressions). The first of these reflected fine-grained changes through time, by grouping Onsets 2–7 into three bins (2,3; 4,5 and 6,7). The second reflected coarse-grained change through time, i.e. across the course of the entire experiment, which was investigated by dividing the experiment into its 3 natural partitions (P1, P2, and P3), representing each block of the experiment for onsets 2:8. Finally, the three-way-interaction (onsets 2:3, 4:5, 6:7 across partitions P1, P2 and P3) combines both habituation and sensitization into one interaction regressor, with one hypothesis reflecting a decrease in sensitization through the course of the experiment. All remaining contrasts, such as the Mean/Intercept and analysis just on Factors (without any temporal component), were performed on onsets 2:8.

2.7. Design Matrices and Mass-univariate analysis

A Mass Univariate Analysis (MUA) was conducted in FieldTrip (Oostenveld et al., 2011) on our ERP data, using FieldTrip's cluster-based permutation test method. The significance probabilities of the permutation tests were calculated using the Monte Carlo method, and all tests were run for 25,000 permutations.

The MUA was performed on what we name the Pattern Glare Index (PGI). As discussed in subsection *Hyper-excitation*, of the Introduction, this index enabled us to focus our study on where the aggravating medium stimulus exhibited more extreme responses than the thin and thick stimuli. These are situations where one might believe hyper-excitation is being observed. The equation used for its calculation was the following:

PGI = medium – mean(thick, thin)

The analysis included regressing the data onto the following predictor variables.

Predictor variable 1: The intercept of the regression model was a predictor variable, with data collapsed across onsets 2–8 and across the entire experiment. Since all regressors entered into the regression model are mean-centred, the intercept becomes the mean of the basic stimulus-effect on the PGI, which identifies data points in which medium is extreme relative to thick and thin.

Predictor Variable 2: The factor scores derived from the factor analysis were used as regressor predictors, with data collapsed across onsets 2–8 and across the entire experiment. The factors were identified as follows: *visual stress, headache,* and *discomfort.*

Predictor Variable 3: Continuous regressors representing the change through time were used as predictors. We considered two different profiles of change through time: *habituation* and *sensitization.* Habituation reflects an exponential decrease, whereas sensitization reflects an exponential increase, given in the following form:

$$Y_{i,sens} = e^{X_i} \quad and$$

$$Y_{i,hab} = e^{(1-X_i)},$$

$$where, i \in N\ (1 \le i \le 3)\ \ s.t. \quad X_i = \frac{(i-1)}{2},$$

$$according\ to\ which \quad X_1 = 0,\ \ X_2 = 0.5,\ \ X_3 = 1$$

Thus, we raise e to the power of a linear decrease in the habituation regressors, and a linear increase in the sensitization regressors. The resulting exponential decrease or increase was selected as neural responses are typically better described by exponential changes, for example, exponential decay is common in biology and neural dynamics (Trappenberg, 2009), reflecting the non-linearity of neuron firing. The regressors, after mean-centring, are visualised in Fig. 4, where *time_point* $i = Y_{i,hab}$ on the left-hand side and *time_point* $i = Y_{i,sens}$ on the right-hand side.

Predictor variable 4: Factor × Time interaction regressors were entered into regression models, where Factor is Headache and Time could be Habituation or Sensitization.

The habituation and sensitization regressors resulted from the following procedure: firstly, for both types of regressors, we generated a baseline-shifted form of each factor, to have a completely positive

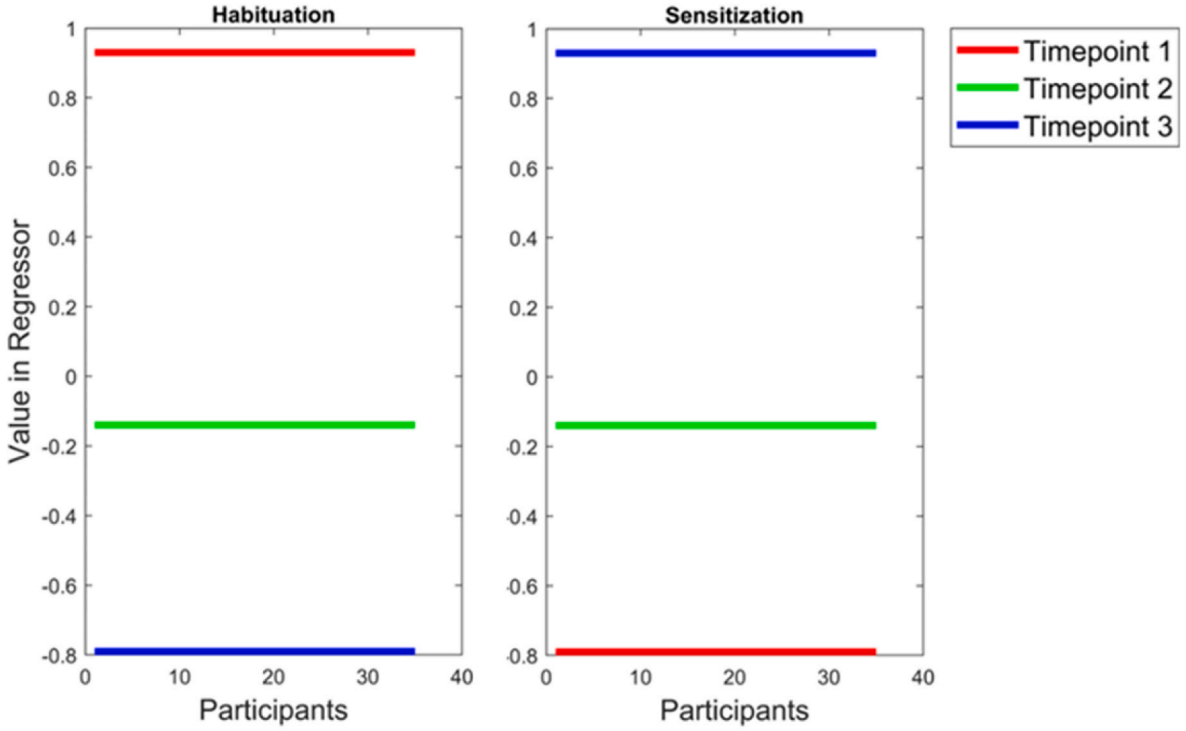

Fig. 4. (Left) A regressor representing habituation through time, (Right) a sensitization regressor representing sensitization through time. The x-axis represents the participants and the y-axis the design matrix value. Please refer to the manuscript online for colour versions of the figure.

regressor. This effectively assumes that participants that scored low on each factor would not habituate or sensitize. We did this by subtracting the minimum (i.e., most extreme negative) score from each participant's score. Then, the baseline-shifted scores were multiplied with the exponential decrease in the habituation case, and the exponential increase in the sensitization case. Lastly, in both cases, the regressor was mean centred.

The resulting Headache x Habituation, as well as Headache × Sensitization interaction regressors are shown in Fig. 1. Thus, in the habituation case (see left side of Fig. 1bi), the resulting interaction regressor reflects the intuition that the greatest differences in brain responses should be observed in the first time-period, with the PGI response being much larger as the score on the factor increases. Then, habituation should mean that differences in brain responses reduce on the second time-period and disappear by the third, leaving all participants with the same low response reflecting the extinguishing of hyper-excitation. (This is not the pure interaction between a factor and habituation since that would not fully reflect our intuition of habituation. In particular, since there is a reduction in hyper-excitation across the course of the experiment, the average response is also reducing through the partitions. However, for presentational ease, we still use the term interaction.) Conversely, in the case of sensitization, the resulting interaction regressor expresses no factor differences at the first time-point, more at the second and finally, the biggest differences at the last.

These two-way interaction regressors, Factor x Time (where Factor is Headache and Time could be Habituation or Sensitization), were applied over both time granularities: Onsets and Partitions.

Predictor Variable 5: Orthogonalized Factor × Time interaction regressors were also tested. This analysis is presented in the Appendix A5.

Predictor Variable 6: Finally, a three-way interaction regressor was entered into the MUA. This regressor represents Headache x Habituation {for Partitions} x Sensitization {for Onsets}.

The three-way interaction regressor contains both the Headache x Habituation {for Partitions} and Headache x Sensitization {for Onsets} regressors described under point 4. The three-way regressor consists of the following. 1) The Headache x Habituation {for Partitions} part involves three partitions, with each partition consisting of all subjects (3 partitions x 32 subjects). 2) Within each partition, there are three groups of onsets: 2; 3, 4; 5 and 6; 7. This results in 9 groups for the three-way-interaction. Once such a column vector is constructed, the procedure described under point 4 is applied to generate the final regressor.

The three-way interaction regressor builds on both the two-way interaction regressors {headache x habituation for partitions} and {headache x sensitization for onsets}. The intuition reflects the hypothesis that, during the course of the experiment, participants exhibit a decreased sensitization through the onsets. Thus, at the beginning of the experiment (partition one), hyper-excitation increases substantially through the onsets and the extent of that increase is dependent upon participants' headache score (higher on headache, more sensitization). This headache by sensitization pattern reduces in partition 2 and then disappears by the end of the experiment (partition 3). Fig. 5 depicts the three-way interaction regressor. Thus, what we see in Partition 1 is similar to what we would observe for the two-way interaction of headache by sensitization for the Onsets. Then, Partition 2 is similar, but with

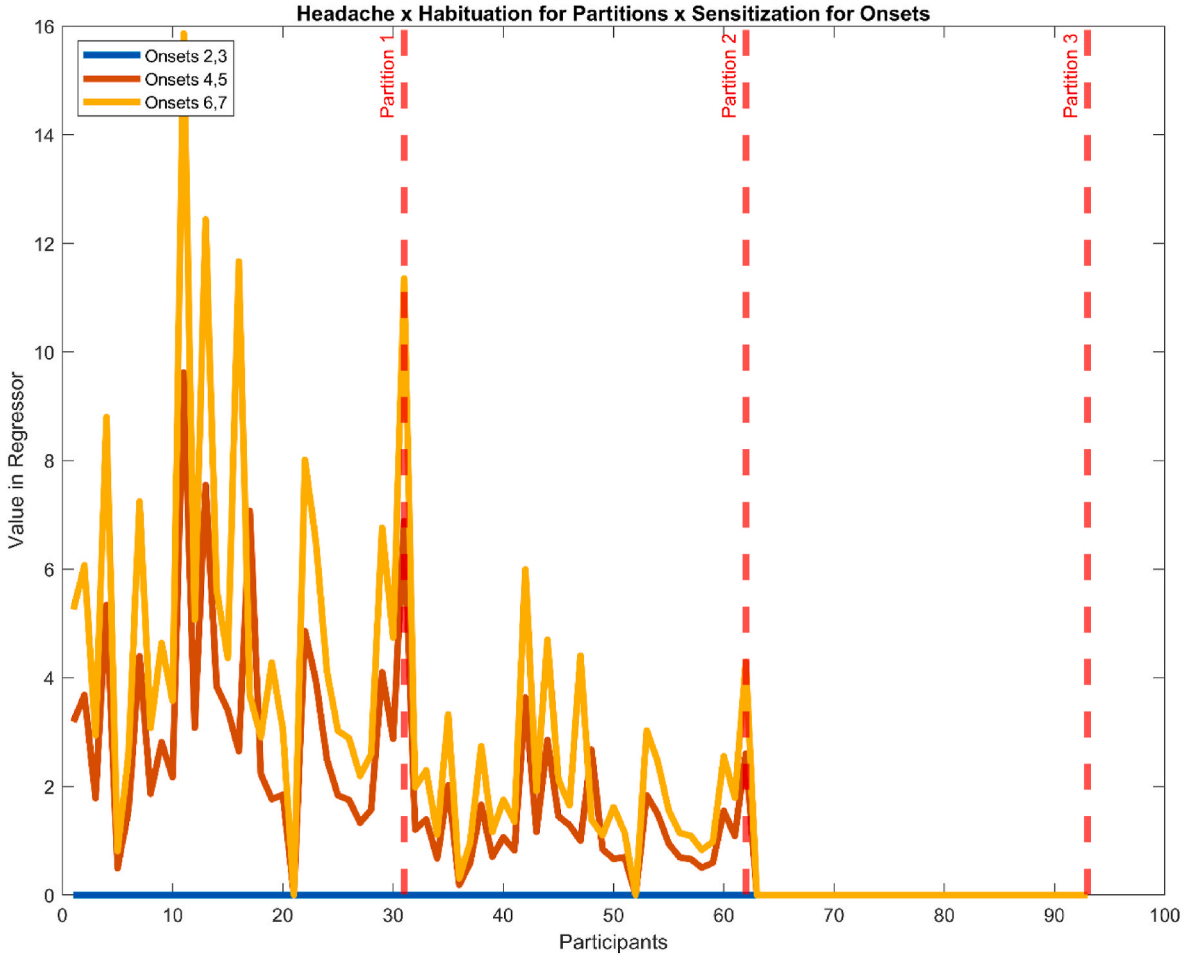

Fig. 5. *Example three-way-interaction regressor for the* Headache x Habituation for Partitions x Sensitization for Onsets effect: *The x-axis represents participants, repeated for each partition. The y-axis indicates the design matrix value assigned. Onsets are indicated by the blue, orange, and yellow lines (2,3; 4,5; 6,7) with partitions segmented by the red dashed lines. (Note, the actual regressor run, would also be mean-centred). Please refer to the manuscript online for colour versions of the figure.*

the headache by sensitization for Onsets pattern "turned-down", i.e., less difference across Onsets (the sensitization) and across participants (headache). Finally, Partition 3 reflects a complete absence of the headache by sensitization for Onsets pattern, i.e., nothing changes across Onsets or participants (headache). Additionally, since there is a reduction in hyper-excitation across the course of the experiment, the average response also decreases through the Partitions.

FieldTrip, the MUA analysis software used, only enables regressions to be formed with an intercept and one other regressor. This is due to the technical difficulties associated with performing the cluster inference permutation test over complex design matrices. Consequently, one is forced to run multiple separate regressions, with different regressors. To respond to this difficulty, we also ran orthogonalized contrasts, the results of which are presented in supplementary material/appendix A5.

The parameters inferred for regressors were statistically examined through two-tailed one-sample t-tests (testing the difference of a single regression coefficient to zero) at the voxel level and we searched for significant clusters (FWE-corrected with $p < 0.05$, cluster-level), with a cluster-forming threshold of 2.5 % (i.e., alpha = 0.025).

2.8. Regions of interest

Similarly, to (Tempesta et al., 2021), we considered the evoked transients observed at posterior electrodes, arising from stimulus-onset. Following (Tempesta et al., 2021), we limited our analyses to a space-time region of interest (ROI) centred around the posterior electrodes. This was selected from the mean/intercept effect (see Results). All (non-intercept) regressors are mean-centred, ensuring that the intercept of the regression becomes the grand mean and is orthogonal to all (non-intercept) regressors. Thus, ROI selection on the mean/intercept does not inflate the type-1 error rate when testing the (non-intercept) regressors in that ROI. We give the full details of this procedure in Appendix/Supplementary Material A6.

We used one-sample t-tests to demonstrate that individual regression coefficients (for our headache, time, headache-by-time, headache-by-time-for-onsets-and-partitions, and intercept regressors) are statistically different from zero. All analyses were run two-tailed.

Additionally, to enable reproducibility of our results, we have included an additional file containing the ROI used in this analysis.

2.9. Data visualisation

MUA finds statistically significant relationships between regressors and space-time ERP maps. This approach does not provide a complete visualisation: for example, it does not show how particular differences between stimuli underlie an effect. We included ERP time-series plots to provide this extra information, placing our participants into two groups based on a median split of headache scores.

A further analysis was developed to select the appropriate channel for visualisation purposes. As part of the MUA, FieldTrip reports a collection of statistics over a 3D matrix, two representing space and one time, including significance levels (p), and t-statistics. The electrode used for visualising ERPs was selected by computing the cumulative count of significant samples/voxels for each channel, i.e. where the significance level was ≤ 2.5 % (i.e., probability of 0.025) at that point in time and space. The electrode with the highest count in a significant cluster was then selected for visualisation.

Following the above electrode selection, 95 % confidence intervals (CI) for each time series were computed using bootstrapping. Firstly, *N* participant ERPs are sampled with replacement, where *N* is equal to the number of participants. Sampling with replacement allows participants to be selected multiple times, or not at all, in each sample thus introducing variability between the samples based on the variation in the original dataset. The grand average of these bootstrapped ERPs for each condition were then computed and stored. This process was repeated 3000 times to create a distribution over participants bootstrapped grand-averaged ERPs. Finally, for each timepoint in the time series, 2.5 % and 97.5 % percentiles were calculated based on the bootstrapped distribution to create confidence intervals around the ERPs.

3. Results

The results that follow are separated into five main components: regressing the PGI onto 1) the Mean/Intercept; 2) Headache; 3) Headache x Time for Partitions interaction regressors; 4) Headache x Time for Onsets interaction regressors; and 5) Headache x Time for Partitions x Time for Onsets interaction regressors. The last of these was conducted because the Headache x Habituation for Partitions and the Headache x Sensitization for Onsets were themselves significant, suggesting a specific three-way interaction. Thus, we only ran the corresponding three-way interaction: Headache x Habituation for Partitions x Sensitization for Onsets; no other three-way interaction was tested. (A 6th pure change through time regressor was also analysed but is reported in a companion paper (Dogan et al., 2025).) The mean and variance of the main variables contributing to the Headache factor are presented in Table 2.

We are most interested in the positive going effects at the occipital electrodes, so the following figures are targeted at those effects. We adopt this focus because the mean/intercept analysis revealed a positive going effect in the occipital area, i.e., over visual cortex, suggesting that the hyper-excitability generated by the medium stimulus manifests as a more extreme response in a positive going direction over visual cortex. Since all our further analyses are carried out in the ROI identified from the mean/intercept, the association of medium with a more extreme positive going pattern is carried over to these further contrasts, i.e., on Headache; Headache x Time for Partitions; Headache x Time for Onsets; and Headache x Time for Partitions x Time for Onsets.

3.1. Mean/intercept effect

MUA found statistically significant clusters for our mean/intercept effect across the whole scalp and through time (within our bounding window from 56 to 256ms: see methods and Appendix/Supplementary Material, subsection A6). This was our statistically strongest effect, and it was mostly present in the occipital area of the scalp, as expected.

In Fig. 6, we can see two figure parts, marked (a) and (b), capturing the effects between 56 and 256ms. Fig. 6(a) shows scalp topography maps through time during our bounding window 56–256ms after stimulus presentation. The topographic plots represent the unthresholded t-values at each time-space sample, with a scale adjusted based on the maximum t-value present in the resulting statistical test. Electrodes belonging to the significant (family-wise error (FWE) corrected) cluster are highlighted in red. These indicate that the effect is mostly at the posterior of the scalp, with the effect lasting between approximately 100 and 256ms. The cluster has a p-value ≤ 0.001 (FWE-corrected, cluster-forming threshold 0.025), with the peak of the effect at 173ms. Fig. 6(b) shows the grand average ERPs for the most continuously significant electrode in the cluster. These time-series are split into two subplots: the top panel displays the PGI, with the panel below showing the individual stimulus conditions (thin, medium, and thick stripes) that contribute to the PGI. The coloured shaded areas represent the 95 %

Table 2
Mean and standard deviation of headache variables used in this analysis (prior to factor analysis).

Variable	Measurement
Headache Intensity	Mean: 5.4 Standard Deviation: 2.52
Headache Duration	Mean: 3.7 Standard Deviation: 6.83
Headache Frequency	Mean: 19.7 Standard Deviation: 28.8

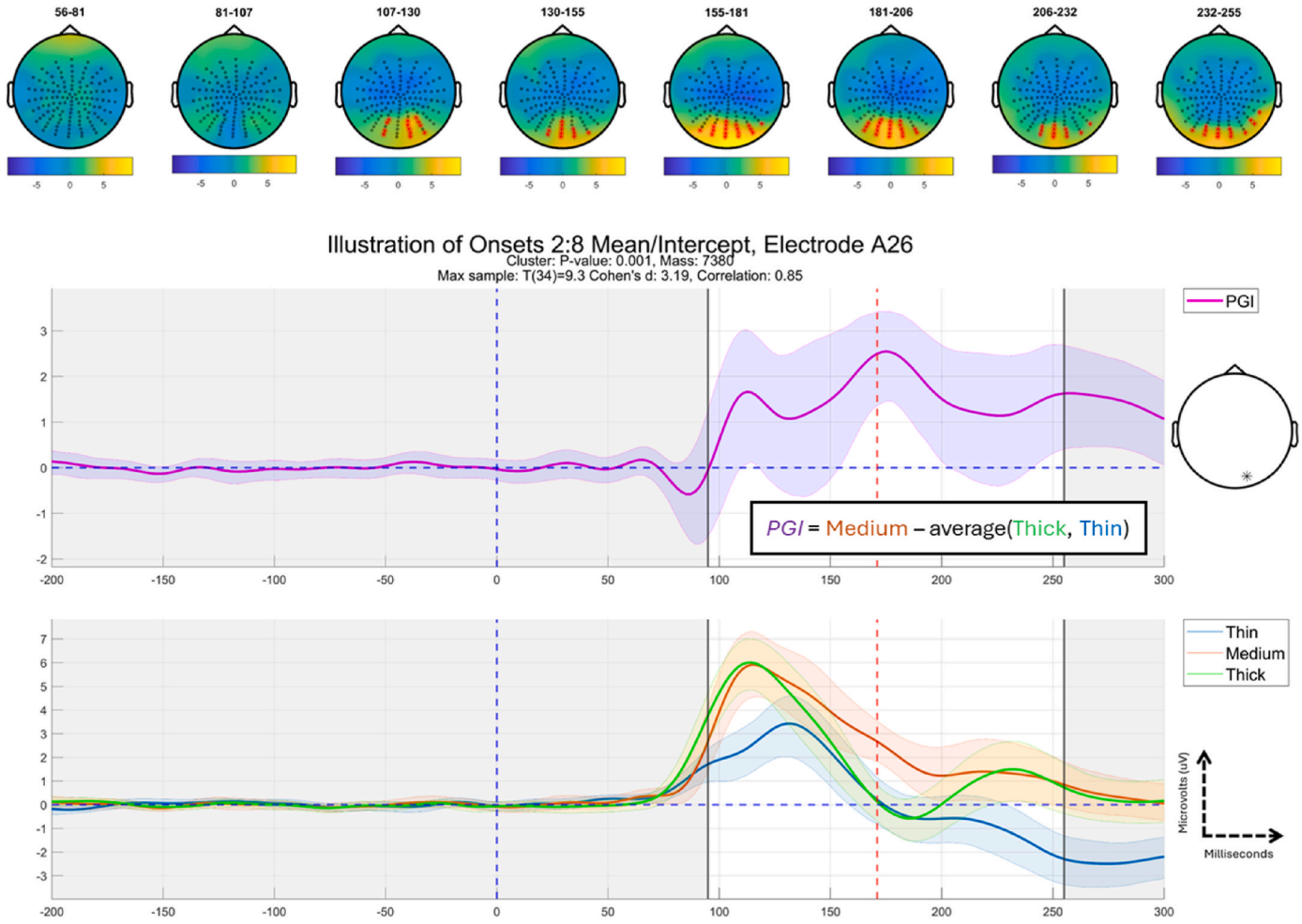

Fig. 6. Mean/Intercept effect: *(a) Topographic maps through bounding time window, 56-256ms after stimulus onset, with intervals of ~25ms. A very strong positive-going cluster is observed at posterior electrodes, while an associated central negative-going cluster is also present, likely reflecting the opposite side of the driving dipole. (b) Grand average time-series of the PGI and individual conditions at the electrode that is the most continuously significant through time. The coloured shaded regions represent 95 % confidence intervals for each time-series. The black lines indicate the start and end of this positive cluster through time, with the red dashed line indicating the peak of the effect. The aggravating stimulus (medium) is clearly stronger than the mean/average of the control stimuli (thick and thin) for an extended time-period, reflecting, we would argue, a time-domain correlate of pattern-glare induced hyper-excitation. Standardised effect sizes are given as Cohen's d and linear correlation. Please refer to the manuscript online for colour versions of the figure.*

confidence intervals.

Table 3 summarises the significant clusters revealed by the MUA for the Mean/Intercept regressor. Both negative and positive tails are included, and the information displayed are the results of the significance test (i.e., probability of arising under the null), the cluster's most sustained electrode, the time of this electrode's peak and t-value of this electrode's peak; and the sum of the t-values across the whole cluster.

Table 3
Collective results for both positive (+1) and negative (−1) tails of the mean/intercept effect. For both the positive and negative going clusters, the following values are presented: the significance probability (p-value, FWE-corrected); the electrode where the effect is most sustained through time; the time of the peak for the most sustained electrode; the t-value at that peak; and the summed t-values of the significant cluster. Clusters are ordered from most to least significant; * indicates $p \leq 0.05$.

Mean/Intercept		
Statistic	*Positive Cluster 1*	*Negative Cluster 1*
p	$\leq$ **0.001***	$\leq$ **0.001***
Most sustained electrode	A26	C24
Time of peak of most sustained	173ms	174ms
Max T(34)-value	9.3	6.8
Cluster Stat	7380	10,155

Consistent with Fig. 6, Table 3 shows two large clusters, the positive-going posterior one we focus on in Fig. 6 and the second negative-going more central cluster, seen in Fig. 6(a) ($p \leq 0.001$; FWE-corrected; cluster-forming threshold 0.025). These suggest a sustained hyper-excitation response to the (aggravating) medium spatial frequency stimulus.

The posterior positive going cluster that we observe here becomes the ROI that we use for all future analyses. We chose to focus on this cluster, since it most directly conformed with our prior hypotheses. Furthermore, although also large, the more central negative-going cluster looks to be the opposite side of the electrical dipole generating the positive cluster. (Indeed, such polarity reversals on the scalp are typically observed when an average reference is taken.) Consistent with this, the size of the negative-going cluster waxes and wanes in synchrony with the positive-going cluster, suggesting that the two effects are strongly negatively correlated. This, in turn, suggests that no more substantive information would be gleaned from also exploring the negative-going effect further.

3.2. Analysis on headache factor

In this section, we present analysis for the Headache factor for all

participants with cluster inference being performed within the ROI identified by the mean/intercept contrast. One significant positive-going cluster was identified for the Headache factor (see Fig. 7) over occipital lobe within the mean/intercept ROI. The effect spanned 125–192ms. The (FWE-corrected) *p*-value is 0.045, with the peak of the effect found at 163ms with a *t(33)*-value of 3.83 (Table 4).

Fig. 8(a) shows the scalp topography maps through time during our bounding window (56–256ms) for the significant cluster. Consistent with Fig. 8(a), the effect starts at 125ms lasting until 192ms, centred over the occipital lobe with the peak electrode being A29. Fig. 8(b) displays the grand average ERPs for the most continuously significant electrode in the cluster divided into high (right column) and low (left column) according to a median split on the Headache factor scores.

This effect suggests a time-domain correlate of pattern-glare induced hyper-excitation that is sensitive to susceptibility to headache as participants in the high group show an increased evoked response to the clinically relevant stimuli, medium.

3.3. Two-way interactions: headache-by-time

These two-way interactions are key contrasts, since they encapsulate how our condition variable (i.e., headache) modulates change through time (habituation or sensitization), and the granularity of time (Onsets or Partitions) at which that modulation manifests. Across the headache factor considered here and other factors considered in the companion paper (Dogan et al., 2025), the only two-way interaction effects that survived FWE correction were Headache-by-Habituation for Partitions and Headache-by-Sensitization for Onsets. We focus first on habituation (see section 3.3.1) and then on sensitization (3.3.2), with all other effects summarised in section 3.5, Table 8.

For each time pattern, there is collinearity between the three relevant interaction regressors. For example, considering habituation across the partitions, after combining the factor scores with the Habituation effect there is strong collinearity, which is largely driven by the Habituation effect being present in all the interaction regressors. Consequently, we present our two-way interaction results for the orthogonalized regressors in the main body of this paper, with the orthogonalized regressors in the supplementary material/appendix (appendix A5). We only present statistically significant results here. Close to-, but not statistically significant, effects are presented in Appendix A5. Additionally, effects that come out in both the orthogonalized and non-orthogonalized analyses can be considered strong. This is because the former of these is the statistically most principled, but the orthogonalization process can distort the regressor. Thus, an effect that also comes out in the absence of orthogonalization is assured to also conform to the intuition we have for our two-way regressors.

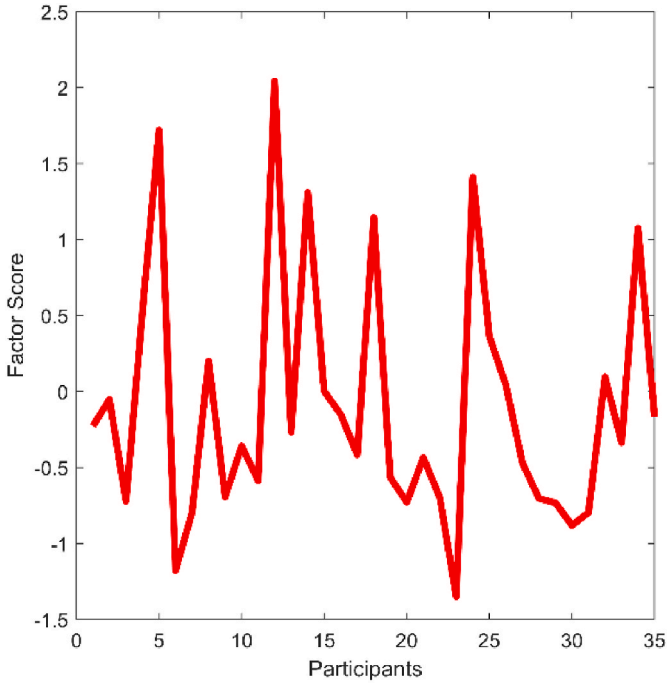

Fig. 7. Headache factor regressor. The x-axis represents the participants and the y-axis the design matrix value assigned to each one.

Table 4
Collective results for the positive (+1) tail for the analysis on the headache factor. For each effect that crossed the cluster forming threshold, the following values are presented: the significance probability (p-value, FWE-corrected); the electrode where the effect is most sustained through time; the time of the peak for the most sustained electrode; the t-value at that peak; and the summed t-values of the significant cluster (i.e., the Cluster stat). Clusters are ordered (left to right) from most to least significant; PC = positive cluster found within the ROI. * Indicates p ≤ 0.05.

Headache Factor		
Statistic	*PC1*	*PC2*
p	**0.045***	0.5908
Most sustained electrode	A29	A28
Time of peak of most sustained	163ms	247ms
Max T(33)-value	3.8	0.8
Cluster Stat	244	21

3.3.1. Headache x habituation for partitions

In this section, we present the non-orthogonalized, Headache x Habituation for Partitions interaction regressor. (The interaction for the Orthogonalized factor was not significant (cluster p = 0.0663) but showed some similar effects to those presented below (see Appendix A5.1, section "Orthogonalized Headache x Habituation for Partitions" for orthogonalized version)). MUA identified one statistically significant positive-going cluster when fitting the Headache x Habituation for the Partitions regressor (depicted in Fig. 9). The (FWE-corrected) *p*-value is 0.0005, with the peak of the effect found at 133ms with t(100) of 3.91 (Table 5).

Fig. 10(a) shows the scalp topography maps through time for the significant cluster, over a range of 56–256ms after stimulus onset. As seen in Fig. 10(b), the effect starts at 110ms and lasts until 195ms, sitting over the occipital lobe, with the "peak" electrode being A29.

Fig. 10(b) displays the grand average time-series for the most continuously significant electrode in the cluster, divided into high and low according to a median split on participant scores on the Headache factor. The middle column depicts the interaction between Low and High groups, focusing on the point marked by the black vertical dashed line in time-series plots.

The upper interaction line-chart plot in Fig. 10(b) (on PGI) shows that we are observing a pattern similar to our characteristic habituation pattern. That is, for the low group, the differences between partitions are smaller and fail to exhibit a consistent change through the partitions (e.g., with the middle partition, P2-PGI, the lowest; see green filled diamond). In contrast, partition one is elevated for the high group (red filled circle). Additionally, while, in our data, we often see full habituation by partition 2 (green filled circle), here there is evidence that the high group does not fully habituate until the 3rd partition (light blue filled circle).

Additionally, the high group (right hand side) in the 2nd row of Fig. 10(b) (i.e. the Medium stimulus plotted alone) shows that the habituation pattern for the Medium stimulus does not last across the full window of significance, i.e. for the first part of the window of significance (from ~110ms to ~150ms) partition 1, 2 and 3 for Medium sit on top of each other. This suggests some involvement of Thick and Thin in the change in PGI through the partitions. The second half of the window of significance (from ~150ms to 195ms) does however show the

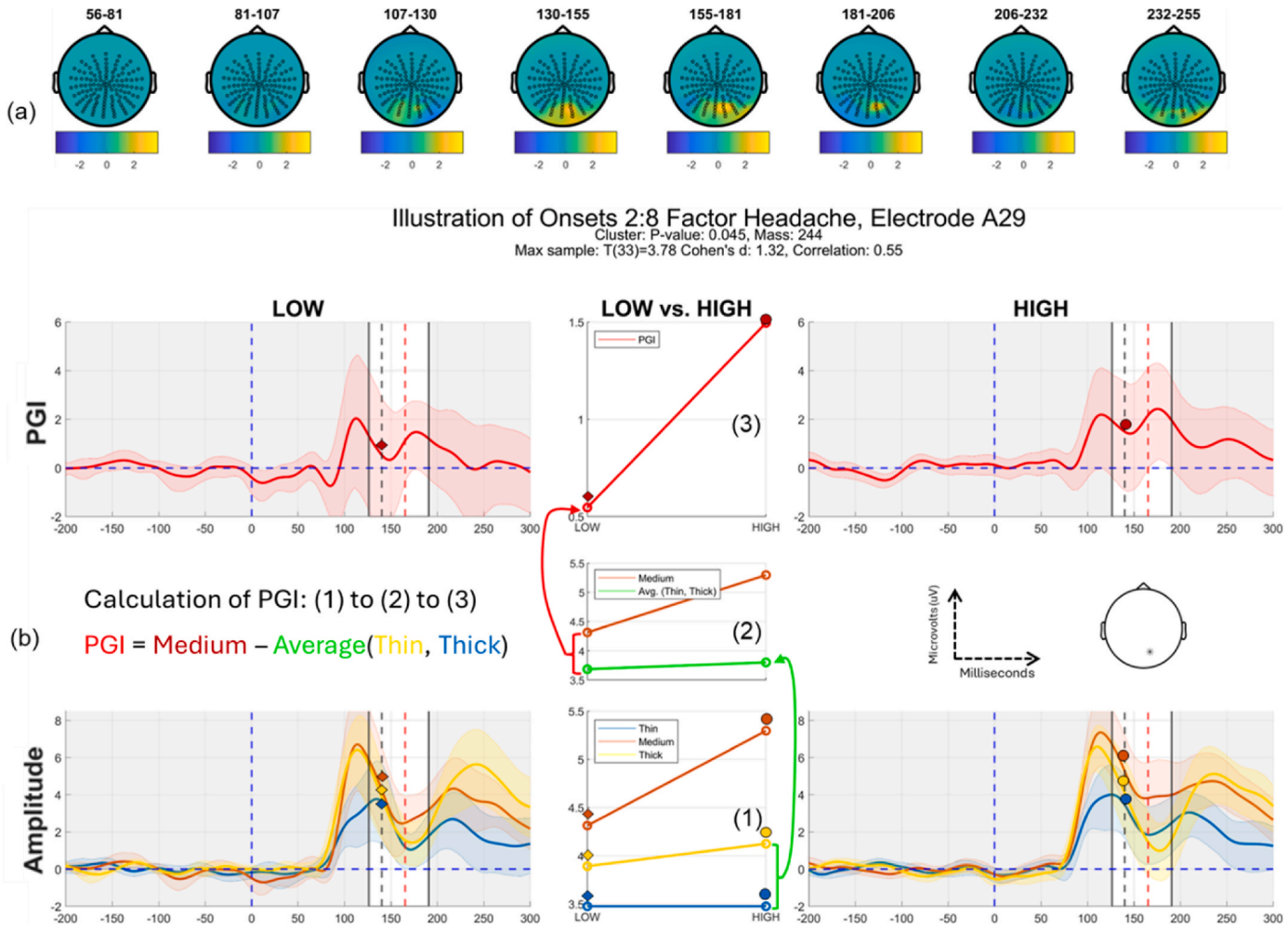

Fig. 8. (a) Topographic maps of significant positive-going cluster in the mean/intercept region-of-interest, illustrating activation from 56 to 256 ms after stimulus onset, with approximately 25 ms intervals between each map. (b) Grand average time-series of the Pattern Glare Index (PGI, top row) and individual conditions (bottom row) at the electrode showing the most continuous significance over time. The left and right columns represent a median split of Headache factor scores into Low and High groups, respectively. The middle column depicts the effect between Low and High groups, focusing on the point marked by the black vertical dashed line in time-series. (b)(1) Amplitudes for Low and High groups for each condition (Thin, Medium and Thick). (b)(2) Low and High groups for the Medium condition and the average of the Thin and Thick conditions. (b)(3) Low and High groups for the Pattern Glare Index (PGI), calculated as the difference between Medium and the mean of Thin and Thick. The shaded coloured regions in each time-series indicate 95 % confidence intervals. Black lines mark the onset and offset of the most significant cluster over time, with the red dashed line indicating the peak of the effect. Within this significant time window, the response to the aggravating stimulus (Medium) is substantially stronger than the average response to control stimuli (Thin and Thick) in the High group, but much less so in the Low group. This extended effect suggests a time-domain correlate of pattern-glare-induced hyper-excitation that varies with susceptibility to headache. Standardised effect sizes are given as Cohen's-d and linear correlation. Please refer to the manuscript online for colour versions of the figure.

Table 5
Collective results for positive (+1) tail of the Headache x Habituation for Partitions effect. For each effect that crossed the cluster forming threshold, the following values are presented: the significance probability (p-value, FWE-corrected); the electrode where the effect is most sustained through time; the time of the peak for the most sustained electrode; the t-value at that peak; and the summed t-values of the significant cluster. PC = positive cluster found within the ROI. * indicates $p \leq 0.05$.

	PC1
p	**0.0005***
Most sustained electrode	A29
Time of peak of most sustained	133ms
Max T(100)-value	3.9
Cluster Stat	945

Table 6
Collective results for the positive (+1) tail of the Headache x Sensitization for Onsets effect. For each effect that crossed the cluster forming threshold, the following values are presented: the significance probability (p-value, FWE-corrected); the electrode where the effect is most sustained through time; the time of the peak for the most sustained electrode; the t-value at that peak; and the summed t-values of the significant cluster. Clusters are ordered (from left to right) from most to least significant; PC = positive cluster found within the ROI. * indicates $p \leq 0.05$.

Statistic	*PC1*	*PC2*
p	**0.005***	0.2572
Most sustained electrode	A28	A28
Time of peak of most sustained	142ms	244ms
Max T(103)-value	4.1	2.9
Cluster Stat	715	34

Table 7
Collective results for the positive (+1) tail of the Headache x Habituation for Partitions x Sensitization for Onsets effect. For each effect that crossed the cluster forming threshold, the following values are presented: the significance probability (p-value, FWE-corrected); the electrode where the effect is most sustained through time; the time of the peak for the most sustained electrode; the t-value at that peak; and the summed t-values of the significant cluster. Clusters are ordered from most to least significant; PC = positive cluster. * indicates $p \leq 0.05$.

Statistic	*PC1*	*PC2*
p	**0.003***	0.786
Most sustained electrode	A29	A29
Time of peak of most sustained	145ms	144ms
Max T(292)-value	4.86	3.3
Cluster Stat	1095	179

habituation pattern we are interested in for the Medium stimulus (see bottom right panel of Fig. 10(b), black dashed line with red, green and blue filled circles). This is nicely reflected in the interaction line plot in the middle of the second row of Fig. 10(b). In that plot, we see an habituation pattern for those high on the headache factor (red above green above blue for filled circles) but not for those low on the headache factor (red above blue above green for filled diamonds).

Thus, these time series suggest hyperexcitation that is specific to the high headache group, which habituates through the course of the experiment. Additionally, the Missing N1 effect on headache reported in Tempesta et al. (2021) and in section 3.2, occurs within the time-space region of the effect presented here. This suggests that what we are identifying here is in some respects a decomposition of the earlier headache effect, showing how it changes across partitions.

3.3.2. *Headache by sensitization for onsets interaction regression*

One significant positive-going cluster was identified for the Headache x Sensitization for Onsets regression (see Fig. 11) over occipital lobe within the mean/intercept ROI (see Fig. 12). This effect spanned 125–215ms. The (FWE-corrected) *p*-value is 0.005, with the peak of the effect found at 142ms with a *t(103)*-value of 4.1 (Table 6).

As seen in Fig. 12(a and b), the effect of interest starts at 125ms lasting until 215ms and sitting over the occipital lobe with the peak electrode being A28. Fig. 12(b) displays the grand average time-series for the most continuously significant electrode in the cluster, divided into high and low according to a median split on the participant scores on the Headache factor. The middle column depicts the interaction between Low and High groups at the time-point marked by the black vertical dashed line.

Focusing on these interaction line-chart plots, in the top row of panel (b), a sensitization pattern is only seen for the high headache group, particularly as an elevated PGI for the final onset pair (6:7). In the bottom row of panel (b), a sensitization pattern is apparent for both Low and High groups. The presence of a difference in pattern through Onset-pairs for PGI (top row of panel (b)), but not for Medium (bottom row of panel (b)), suggests that changes in Thin and Thick are contributing to this effect. (Note, this unorthogonalized version of this interaction regressor, has a change in mean amplitude across Onset-pairs built into it. Consequently, even if the headache pattern does not fit well, an effect can be carried by simple change in mean amplitude across Onset-pairs. This might particularly be what is driving the effect at the time-point of our dashed black vertical line. We consider this issue further in the Discussion.)

3.4. *Three-way interaction: headache x habituation (for partitions) x sensitization (for onsets)*

The Headache x Habituation (for Partitions) x Sensitization (for Onsets) interaction was conducted specifically to see whether we could connect the two-way interactions that we have observed: Headache x Habituation (for Partitions) and Headache x Sensitization (for Onsets). Could we find evidence that the sensitization effect we observed for Onsets, habituates across the course of the experiment (i.e., across Partitions)? We did not test any other three-way interactions. Only the unorthogonalized three-way interaction came out as significant. (The

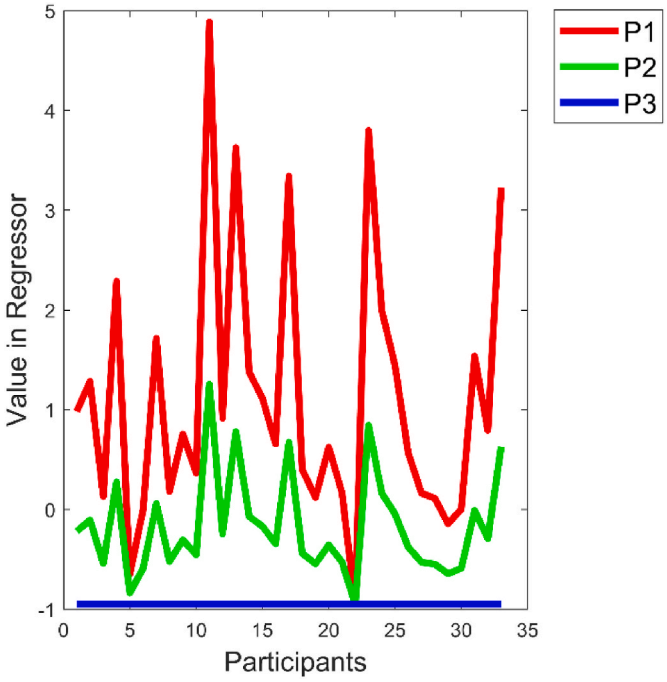

Fig. 9. Headache x Habituation for Partitions interaction regressor. The x-axis represents the participants and the y-axis the design matrix value assigned to them for each partition. Partitions are indicated by P1, P2 and P3. Please refer to the manuscript online for colour versions of the figure.

Table 8
Summary of statistically significant clusters across both time granularities (onsets and partitions) and directionality (habituation and sensitization). The Pure Time contrasts exhibit a change through time, without crossing with the Headache factor; see Fig. 4; thus, they could be considered as Main Effects of the analysis. (The details of the Pure Time contrast are presented in a companion paper (Dogan et al., 2023).) "No cluster found" indicates no clusters formed, i.e., no samples crossed the first level (cluster-forming) threshold. "Non-significant cluster" indicates that there were samples (time-space points) that crossed the cluster-forming threshold, but the resulting clusters did not survive second-level family-wise error correction.

	Partitions		Onsets	
Contrast	Habituation	Sensitization	Habituation	Sensitization
Pure Time Effect	Non-significant cluster (see Dogan et al., 2023)	No cluster found	No cluster found	No cluster found
Headache x Time (unorthogonalized)	Significant Cluster Found (see results, Fig. 10)	No cluster found	No cluster found	Significant Cluster Found (see results, Fig. 12)
Headache x Time (orthogonalized)	Non-significant cluster (see A.5.1 in appendix)	No cluster found	No cluster found	Significant Cluster Found (see A.5.2 in appendix)

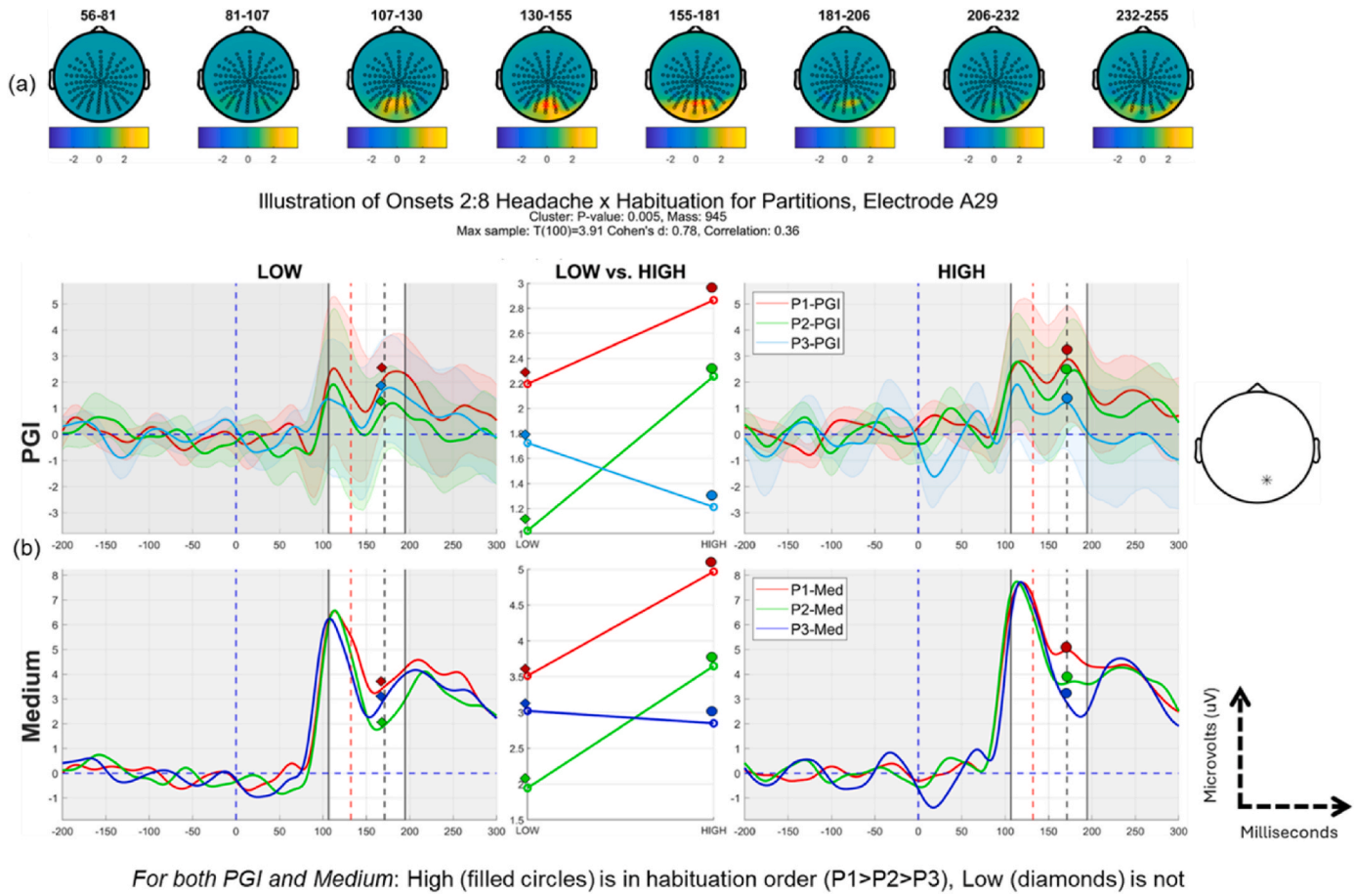

Fig. 10. (a) Topographic maps from 56 to 256 ms after stimulus onset, with approximately 25 ms intervals. A positive-going cluster appears at posterior electrodes, especially between 110 and 185 ms. (b) Grand average time-series of the Pattern Glare Index (PGI) and Medium condition at the electrode with the most continuous significant signal over time. Participants were split into Low and High Headache groups (left and right columns, respectively). The middle column depicts the interaction between Low and High groups, focusing on the point marked by the black vertical dashed line. Shaded coloured regions indicate 95 % confidence intervals. Black lines mark the start and end of the most significant cluster, and the red dashed line shows the peak of the effect. Top row of panel (b) shows PGI and bottom row shows effect on Medium stimulus. In both rows, P1, P2 and P3 represent the three partitions. In the High Headache group (right side of panel (b)), there is a pattern of habituation (an ordered reduction in response) that is absent in the Low group (left side). This habituation effect is clearest in the top row of panel (b), with the largest drop in response between the second and third partitions, suggesting a reduction in hyper-excitation as the experiment progresses. The second row of panel (b), which shows only the medium condition, exhibits a similar trend, although not at the start of the period of significance. This indicates that the Thin and Thick conditions may contribute to the significance of the cluster at its start, see main body of text for further details. Standardised effect sizes are given as Cohen's d and linear correlation. Please refer to the manuscript online for colour versions of the figure.

non-significant orthogonalized version of this contrast is presented in Appendix A5.3).

One significant-positive going cluster was identified for the Headache x Habituation (for Partitions) x Sensitization (for Onsets) effect; see regressor in Fig. 13. The effect sits over the occipital lobe within the mean/intercept ROI. The effect for the most positive going cluster spanned 105–256ms. The (FWE-corrected) *p*-value is 0.003, with the peak of the effect found at 137ms, with a *t(292)*-value of 4.86 (see Table 7).

Fig. 14(a) shows the scalp maps through time during our bounding window (56–256ms after stimulus onset) for the significant cluster. As seen in Fig. 14(b), the effect starts at 105s lasting until 256ms, positioned over the occipital lobe with the peak electrode being A29.

Fig. 14(b) displays the grand average time-series for the most continuously significant electrode in the cluster, segmented into high (right-side) and low (left-side) according to a median split on the participant scores for the Headache factor. The middle column depicts the interaction line-chart between Low and High groups, at the point marked by the black vertical dashed line.

Focusing on these interaction line-charts, there is evidence of a strong two-way interaction for partition 1, see panel [A], driven by the high group showing a (higher amplitude) strong sensitization effect. Accordingly, the response increases 2:3, 4:5, 6:7 through Onset-pairs for the high group (see filled coloured circles on right of plot), which it does not for the low group (see filled coloured diamonds on the left of plot). This two-way interaction is weaker for partition 2, see panel [B]. It is also somewhat weaker for partition 3, than for partition 1: compare panel [A] and [C]. However, the difference in two-way interaction between partitions 3 and 1, is not as big as between partitions 2 and 1. Thus, we do not see as much habituation by the third partition, as we might have expected to see.

It is important to realise that the visualisations of an effect we present with time-series and line-charts (in (b) panels) is not exactly the same as the actual interaction run. We discuss this further in the Discussion; subsection 4.4. This may be why we see a strong three-way interaction, but our visualisation of it is not as compelling as it could be.

Although not a perfect match, the effect we present in Fig. 14 exhibits some overlap with the space and time of the Headache x Sensitization for Onsets effect (Fig. 12) and the Headache x Habituation for Partitions effect (see Fig. 10). This suggests that the three-way interaction we observe in Fig. 14 is part of the same phenomenon that generates the two two-way interactions, i.e. it is a decomposition of the two-ways.

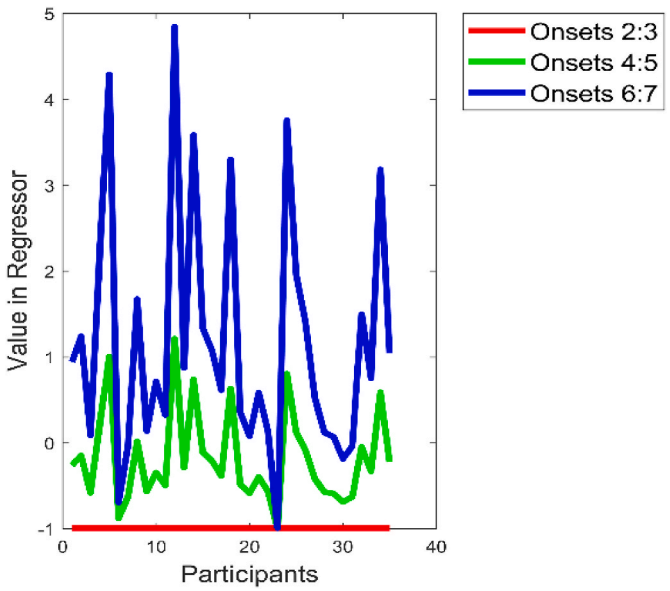

Fig. 11. Headache x Sensitization for Onsets regressor. The x-axis represents the participants and the y-axis the design matrix value assigned to them for each Onset. Please refer to the manuscript online for colour versions of the figure.

3.5. Summary of contrasts

Table 8 summarises the temporal effects we observed and failed to observe. The orthogonalized effects shown in this table are presented in the appendix. Additionally, the orthogonalized three-way interaction for Headache x Habituation through the Partitions x Sensitization through the Onsets is also presented in the appendix (section A5.3). In our results section, we have focussed on sensitization through the onsets and habituation through the partitions. However, we did also explore the opposite patterns: habituation through the onsets and sensitization through the partitions, and importantly, as shown in Table 8, no effects (even just crossing the first level threshold) were found for these alternative patterns of change through time. This adds credence to our position that the dominant pattern in our data is short-term sensitization (through onsets), accompanied by longer-term habituation (through partitions).

4. Discussion

We based our analyses on four main research points about the electrophysiological correlates of pattern-glare in relation to headache susceptibility. We discuss how each of these points stands in the light of our findings.

4.1. Mean/intercept and headache (main) effects (point/contrast 1)

Mean/Intercept: As shown in Fig. 6, across the whole group of participants, we see a sustained highly-significant "hyper-excitation" effect. Medium is above the average of Thick and Thin throughout this single cluster, suggesting that the effect is driven by an elevated response to Medium, consistent with prior research (Wilkins, 1986; Schoenen et al., 1995; Gerber and Kropp, 1995; Tempesta et al., 2021). The effect is most potent in the occipital lobe, centred at A26, lasting effectively from the start of the onset transients (~100ms) to the end of the analysis segment (256ms) and, in fact, beyond segment end; see (Jefferis et al., 2024). There are two effect peaks, one around 120ms (coinciding with the P1) and the other around 180ms (coinciding with the following N1); see Fig. 6(b) top panel.

This finding may relate to previous MEG (Adjamian et al., 2004) findings. Adjamian et al. (2004) detected (broadband gamma) oscillatory correlates of hyper-excitation over the visual cortex of a healthy group of participants, with gratings close to the spatial frequency of our Medium stimulus eliciting the highest increase in power. Further work should attempt to relate our time domain and Adjamian et al.'s frequency domain effects. For example, do the amplitudes of these two effects correlate across participants?

For our findings, a potential confound that it is important to exclude is the possibility that the evoked response effects that we observe are due to eye movements. A detailed analysis on the eye electrodes (VEOG/HEOG) is included in Appendix 1 "Ruling out eye confounds".

Factor main effect: We also observed an effect directly on the Headache factor; see Fig. 8, which is significant, but considerably weaker than the Mean/Intercept effect. This sensitivity to Headache susceptibility is found during the second peak of the Mean/Intercept, around 180ms after stimulus onset, during the first negativity. This effect suggests increased hyper-excitation (i.e., pattern-glare index) for those more susceptible to have headaches. This finding is broadly consistent with previous findings that migraineurs exhibit higher amplitude early visual-evoked potentials (Oelkers et al., 1999). As discussed in more detail in (Tempesta et al., 2021), two studies have previously measured ERPs in a headache prone population using pattern-glare-like stimuli. Fong et al. (2020) found differences between migraine sufferers and controls at around 200- and 400ms post stimulus onset. Their migraine group showed greater negativity at 200ms for high-frequency gratings (13 c/deg). Indeed, their main findings were on the high-frequency grating, while in contrast, the findings we report here occur with the clinically relevant, medium-frequency grating (3 c/deg). However, as elaborated in (Tempesta et al., 2021), it is difficult to compare our effects to Fong et al.'s. This is because Fong et al. did not use repeated onsets and so could not observe an analogue of the effects reported here, which are across Onsets 2 to 8, during which time, unlike our Onset 1 and Fong et al.'s study, the stimulus presented is completely predictable.

Furthermore, Haigh et al. (2019) found larger amplitude N1 and N2 ERP components in a migraine group viewing chromatic gratings. These enlarged responses were associated with higher discomfort ratings when viewing the stimuli.

Comparison to Tempesta et al.: The mean/intercept reported here corresponds to the mean/intercept effect observed in (Tempesta et al., 2021); and there is no surprise that we observe this again, since we are analysing the same data. However, the effect here is larger, because Fieldtrip enables a more appropriate cluster inference for EEG data, where a first-level (cluster-forming) threshold can be set at 0.025, rather than the 0.001 required in SPM (Flandin and Friston, 2017). The signal in scalp-EEG tends to be relatively low amplitude, but broad in space and time (i.e., smooth). SPM's 0.001 first level threshold tends to be too strict to detect such low amplitude-broad effects.

Additionally, our analysis on the (pure) headache factor (a main-effect in the design) also repeats an analysis presented in (Tempesta et al., 2021), with the same data. This headache factor effect was significant in Tempesta et al. ($t(30) = 3.34$, $p = 0.047$, FWE cluster-level corrected, with Random Field Theory and small volume correction), and similarly so in this paper ($p = 0.046$, see details in Table 4).

However, all the interaction effects that we report in this paper are new analyses. Thus, the key original contribution of this paper is the identification of profiles of change through time, i.e., habituation and sensitization, and how those profiles interact with Headache susceptibility.

One aspect of the (Tempesta et al., 2021) findings was the demonstration of increased temporal jitter for the Medium stimulus for those high on the headache factor. It is a possibility that the interaction effects we observe reflect changes in temporal jitter over fine (across onset-pairs) and coarse (across partitions) timeframes for those high on the Headache factor. However, confirming this is challenging, since calculation of phase coherence is impacted by changes in power, and we do indeed observe such changes through the course of our experiment.

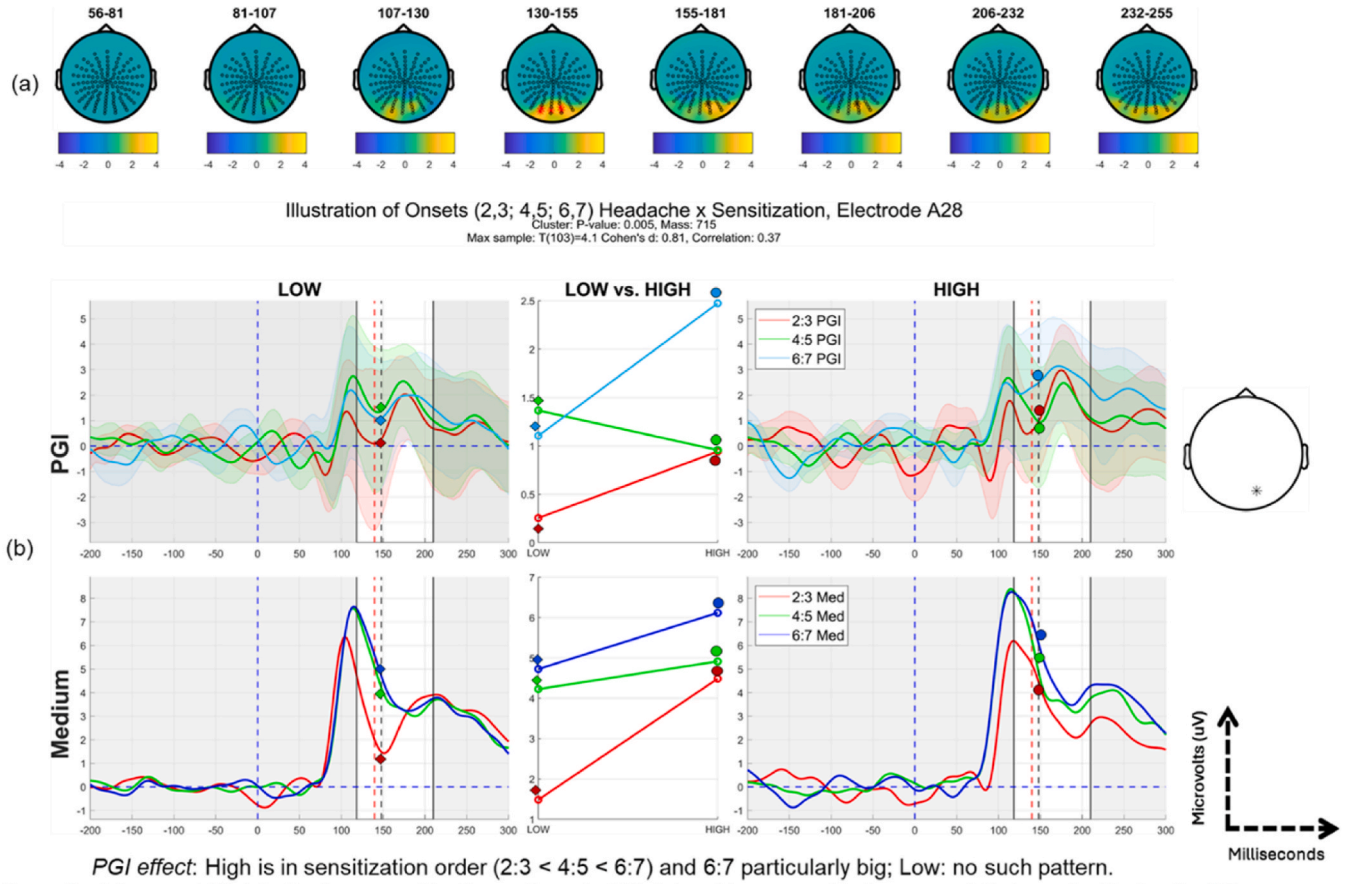

Fig. 12. Headache x Sensitization for Onsets effect: (a) Topographic maps from 56 to 256 ms after stimulus onset, with approximately 25 ms intervals, showing a positive-going cluster at posterior electrodes. (b) Grand average time-series of the Pattern Glare Index (PGI) and Medium condition at the electrode with the most continuous significant effect over time. Participants were split into Low and High Headache groups (left and right columns, respectively). The middle column provides interaction line-chart plots between Low and High groups, focusing on the point marked by the black vertical dashed line. Shaded coloured regions indicate 95 % confidence intervals. Black unbroken lines mark the start and end of the most significant cluster, and the red dashed line shows the peak of the effect. Top row of panel (b) shows PGI and bottom row shows effect on Medium stimulus. In both rows, 2:3, 3:4 and 5:6 represent the three Onset pairs. Now focusing on the interaction line-chart plots in the middle of panel (b). In the top row of panel (b), a sensitization pattern is only seen for the high headache group, particularly as an elevated PGI for the final onset pair (6:7). In the bottom row of panel (b), a sensitization pattern is apparent for both Low and High groups. The presence of a difference in pattern through Onset-pairs for PGI (top row of panel (b)), but not for Medium (bottom row of panel (b)), suggests that changes in Thin and Thick are contributing to this effect. Standardised effect sizes are given as Cohen's d and linear correlation. Please refer to the manuscript online for colour versions of the figure.

4.2. Headache by habituation for partitions interaction effect (point/contrast 2)

Our second finding suggests that this hyper-excitation over the visual cortex decreases (i.e., habituates) through the course of the entire experiment; see Fig. 10. Furthermore, this decrease is modulated by headache susceptibility, with those high on the Headache factor habituating more. This effect suggests brain adaptation on a relatively macroscopic temporal frame, as it was demonstrated over the experiment's blocks that lasted for 10–12 min each.

This finding answers the second hypothesis/question that we identified in the Hypotheses subsection of the Introduction and demonstrates the brain's ability to habituate to an aggravating visual stimulus. Evidence of habituation occurring in the visual cortex already exists (Obrig et al., 2002; Schoenen et al., 1995)) and in some cases, the presence of habituation was also discovered for migraine sufferers (Khalil, 2000; Omland et al., 2016). However, a conflict exists between studies, as previous work has suggested that migraineurs do not habituate (Adjamian et al., 2004; Schoenen et al., 1995). We shortly return to the question of why we observe the particular pattern of change through time that we do; see subsection 4.6. "Potential Explanation of Findings".

Finally, it is important to also acknowledge that this Headache-by-Habituation for partitions effect is only significant unorthogonalized; see Table 8. Consequently, this is an effect where replication is certainly required.

4.3. Headache by sensitization for onsets interaction effect (point/contrast 3)

As shown in Fig. 12, we have obtained evidence for a sensitization effect arising from stimulus repetition that is differentially present for participants susceptible to headaches. This suggests that repeated presentation of a pattern-glare stimulus, with repetition onsets spaced by around 4 s, drives hyper-excitation in the brain to increase through these repetitions for headache sufferers. This is consistent with the first hypothesis we highlighted in the Hypotheses subsection in the Introduction.

Mickleborough et al. (2014) conducted an experiment in which a series of visually complex images were presented to a population of clinically defined migraineurs and healthy participants. Similar to our findings, participant ERPs for the migraineurs relative to the healthy participants exhibited sensitization quickly after stimulus onset, for the duration of the experiment. This sensitization was present for the initial blocks, however, at later stages during the experiment, migraineur's

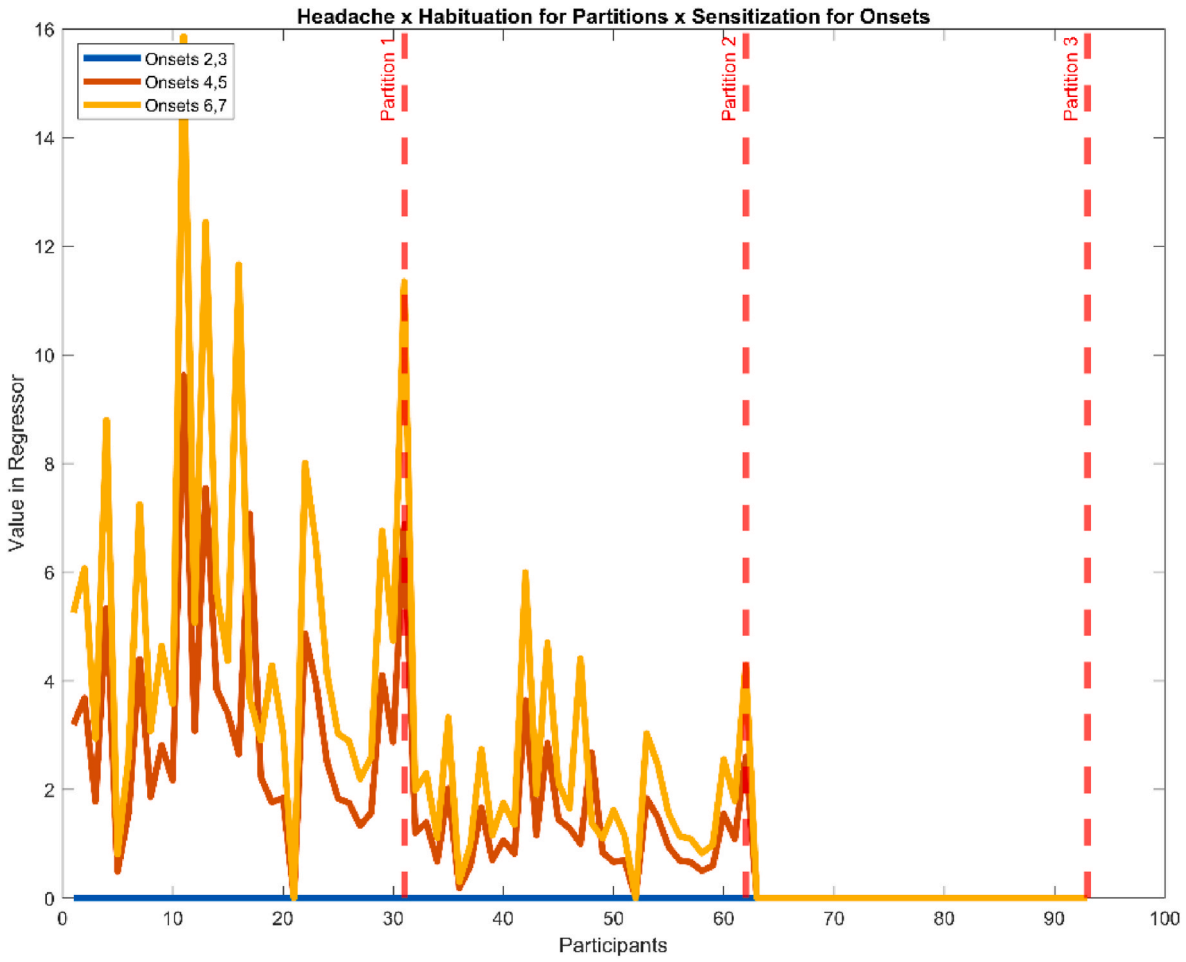

Fig. 13. (Unorthogonalized) Headache x Habituation (for Partitions) x Sensitization (for Onsets) effect: (a) The x-axis represents participants, all of which appear three times, once for each partition. The y-axis represents the design matrix value assigned to each participant for each onset in each partition. Onsets are indicated by the blue, orange, and yellow lines (2:3; 4:5; 6:7) with partitions segmented by the red dashed lines. Note, in the final partition (number 3), the red and blue lines are "under" the yellow line. (Note, a further mean centring would be applied to this regressor.). Please refer to the manuscript online for colour versions of the figure.

ERPs started to show a habituation effect. It is important to highlight that, unlike our experiment in which we recruited from the general population and recorded self-report headache susceptibility, the participants employed by Mickleborough et al. were clinically confirmed migraineurs. Additionally, the experimental paradigm used by Mickleborough et al. is much shorter in overall duration, which may explain why sensitization is present throughout the entire experiment. Finally, since this effect was significant for both the orthogonalized and unorthogonalized contrasts (see Table 8), with identified-clusters that strongly overlap in space and time, it may be that this effect is more reliable than the Headache-by-Habituation for partitions effect reported in the previous subsection. Although, this Headache-by-sensitization for Onsets effect, may not be as clean, as Thick and Thin may be contributing to it; see caption of Fig. 12 and discussion of that figure in the main text.

4.4. Headache-by-habituation for partitions by-sensitization for onsets interaction effect (point/contrast 4)

Because both the Headache-by-habituation for partitions and the Headache-by-sensitization for onsets interactions were significant, with similar scalp topographies and overlap in time, a natural next question is whether these two two-way interactions interact with one another. To explore this, we specifically looked at the Headache-by-habituation for partitions by-sensitization for onsets interaction effect.

Consequently, we have found evidence for the possibility that (differentially) for headache sufferers, hyper-excitation increases through repetition of onsets when they first start viewing pattern-glare stimuli. However, the brains of these participants habituate, leading to reduced hyper-excitation, over a longer time period. This raises the possibility that those high on the Headache factor are aggravated, i.e., hyper-excited, by repeated presentation when they start the experiment, but that aggravation through repetition dissipates for the rest of the experiment. This pertains to the third hypothesis identified in the Hypotheses subsection of the Introduction.

However, we do wish the reader to consider this three-way interaction with some caution. While the p-value for this effect is small ($p = 0.003$), it is not the cleanest of our findings. This is especially with respect to the visualisation of the effect in Fig. 14(b), where the partition three two-way interaction is not as weak as might be expected. As we discuss in section 3.4, it is important to acknowledge that the basing of our time-series and interaction line-chart plot visualisations on median splits, means that they are not a perfect representation of the three-way interaction run. This is because the actual three-way interaction run is based upon a continuous regressor, a point we elaborate on in subsection 4.8. Additionally, this three-way interaction was fundamentally exploratory in nature, i.e. to explore an hypothesis arising from our two two-way interactions. Thus, it definitively needs replication before it can be considered a robust finding, especially, since the possibility of double dipping is present, as the three-way is not completely orthogonal to the two-ways (Bowman et al., 2020; Brooks et al., 2017).

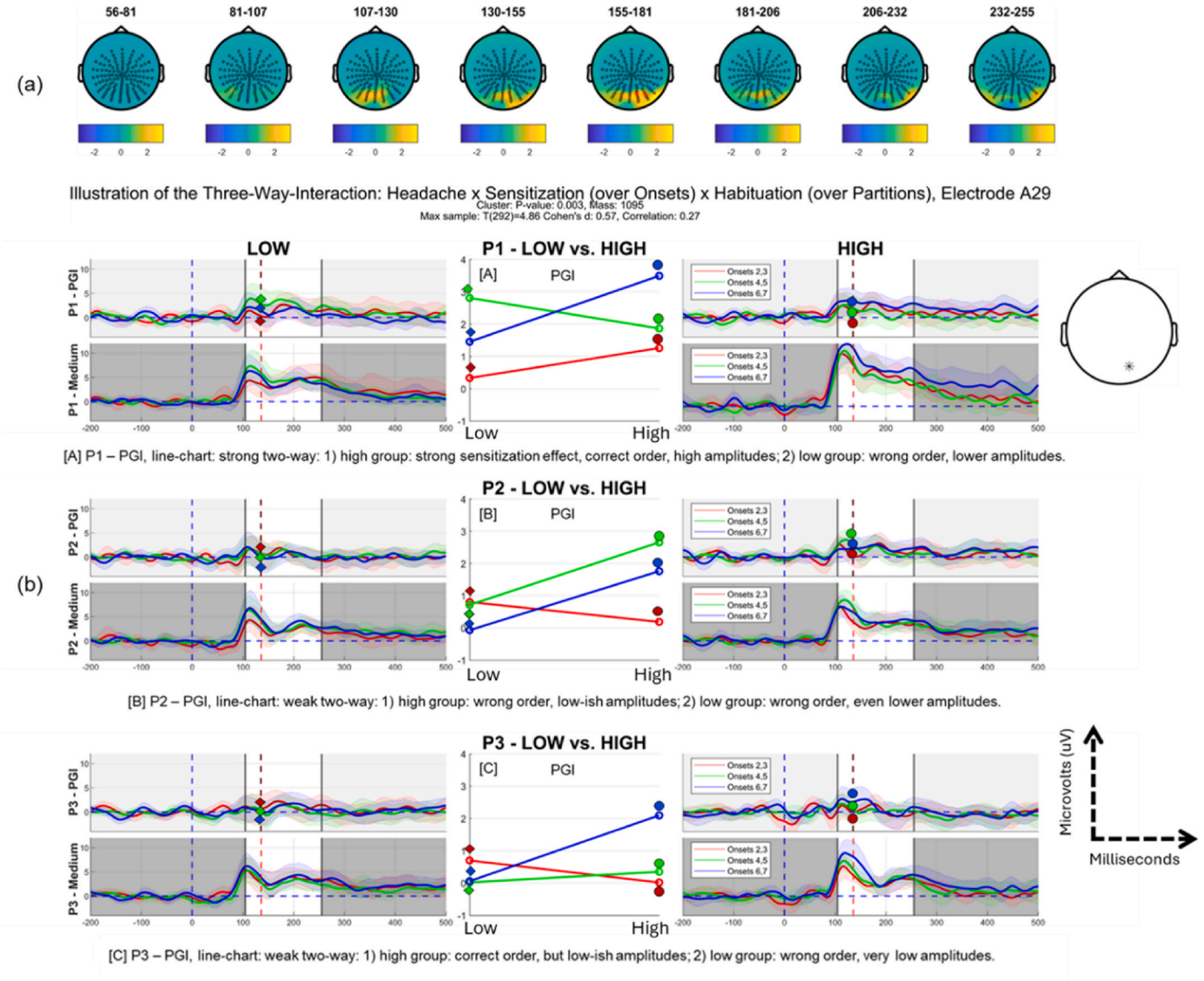

Fig. 14. This figure illustrates the interaction effect of Headache, Habituation (across Partitions), and Sensitization (across Onsets). (a) Topographic maps display positive-going clusters observed at posterior electrodes in the 105–256ms time window, with approximately 25 ms intervals between each map. (b) The grand average time-series of the Pattern Glare Index (PGI) and the Medium stimulus is shown at the electrode with the most continuous significant effect over time. Participants are split by Headache factor (Low on the left, High on the right), and the middle column depicts interaction line-charts, highlighting the time-point marked by the black vertical dashed line. These line-charts are just for the PGI (for simplicity of presentation, we do not show interaction line-charts for the Medium stimulus). The unbroken black lines indicate the start and end of the significant cluster, while the red dashed line marks the peak effect. Rows in light grey show PGI results, and rows in dark grey show the Medium stimulus across three partitions (Partition 1: first two rows, Partition 2: middle two rows, Partition 3: last two rows). Each of these plots show onsets-pairs: 2:3, 4:5, and 6:7, distinguished by colour. The PGI rows (light grey) in panel (b) provide some evidence of a differential pattern across partitions and headache groups. Focusing on the interaction line-charts, there is evidence of a strong two-way interaction for partition 1, see panel [A], driven by the high group showing a (higher amplitude) strong sensitization effect. This two-way interaction is weaker for partition 2, see panel [B]. It is also somewhat weaker for partition 3, than for partition 1: compare panel [A] and [C]. However, the difference in two-way interaction between partitions 3 and 1, is not as big as between partitions 2 and 1. It is important to realise that the visualisations of an effect we present with time-series and line-charts (in (b) panels) is not exactly the same as the actual interaction run. We discuss this further in the main-body of the text. Standardised effect sizes are given as Cohen's d and linear correlation. Please refer to the manuscript online for colour versions of the figure.

4.5. *Formulation of interaction regressors*

There are subtleties to our interaction regressors. This is because they involve two aspects, i.e., for those higher on headache, there should be, (i) more *change through time* (i.e., habituation or sensitization for Partitions or Onsets); and (ii) *larger amplitudes*.

Importantly, because our interest is in hyper-excitation, one does need the second aspect, as well as the first. For example, for Headache by Habituation over Partitions, we do not just want to know that those higher on Headache show more of a reducing pattern across partitions (which might go from positive to negative), we also want to know that this reflects a dissipation of excitation *towards zero*, i.e., that the habituation is from an extreme amplitude down to zero. This is, for example, apparent in panel (bi) of Fig. 1, where the average value (across time-points) in the regressor is only at baseline (i.e., −1) for the lowest participant on Headache (see participant 22, for whom, red, green, blue is all at −1), but this average value increases as one progresses up the Headache regressor.

As an example of this, consider Fig. 12(b), interaction line-chart for PGI in middle of top row. The mean across Onset-pairs for those low on

Headache (three coloured diamonds) is lower than the mean across Onset-pairs for those high on Headache (three coloured filled circles). This amplitude difference between High and Low also contributes to making this a big effect, and it does so in addition to the change through time that we see, i.e. a clearer sensitization pattern for High than for Low.

Although the three-way is more complex, involving two patterns of change through time, these two aspects, change through time and larger amplitudes, are also both inherent to this three-way pattern.

4.6. Potential Explanation of Findings

First negativity: all our effects involving the Headache factor (i.e., the Headache factor on its own; Headache-by-habituation for partitions; Headache-by-sensitization for onsets; and Headache-by-habituation for partitions by-sensitization for onsets) are largest at A28 or A29, i.e., effectively the same point on the scalp. Additionally, there is considerable overlap between the temporal windows of these effects, with a window from ~140ms to ~190ms common to all effects. This suggests that all these Headache effects are really arising from the same features in the data, and potentially the same source(s) in the brain. As further discussed in (Tempesta et al., 2021), this time and space region seems to coincide with a negativity in the raw ERPs, which is particularly evident in the Thick condition (see Fig. 6(b) lower panel), but typically not in the PGI plots, since they represent a contrast of raw ERPs.

This negativity can, for example, be observed in the lower row (Medium stimulus) of panel (b) of Fig. 10, reaching its minimum around 180ms. Furthermore, the effects we observe are often associated with the Medium condition exhibiting a much shallower (or even absent) negativity or a change in this negativity through time; see Fig. 10(b) lower rightmost panel, blue, green and red filled circles. Further work needs to be performed, to understand the brain correlates of this negativity and its relationship to feedforward and/or feedback processing in visual cortex.

Change through time: Why, then, do we observe the particular pattern of sensitization and habituation that we have reported? A number of points can be made.

1. Sensitization over onsets: perhaps the most expected and also strongest effect we observe is sensitization for those high on the headache factor, for the finer time granularity (i.e., onsets), suggesting, a potential deficit in inhibitory mechanisms to control stimulus-driven excitation in striate cortex.
2. Habituation over partitions: a more surprising, but perhaps more intriguing, finding is that hyper-excitation seems to habituate through the course of the experiment. This suggests a successful dampening of hyper-excitation over a long enough period of time for our headache sufferers. However, it is important to remember that our cohort is not clinically selected, and thus may not contain extreme headache sufferers, or only a small number if present. Basically, even for those high on the Headache factor, we may be looking at a relatively well-functioning brain. Consequently, it may not be surprising that their visual systems do successfully habituate. Future work should validate this effect on a clinical group of headache/migraine sufferers. Indeed, it may be that those with extreme sensitivity to pattern-glare stimuli, do not habituate over the course of the experiment or may even sensitize, i.e., with correlates of hyper-excitability increasing through the course of the experiment.
3. Lack of habituation in individuals with low scores on the headache factor (see Fig. 10(b), both rows—PGI and Medium, coloured diamonds): the lack of habituation for those low on the headache factor may reflect that they have less to habituate, i.e., less hyper-excitation in the first place. That is, this does not necessarily imply that they cannot habituate; it is more that they do not have to.

4.7. Robustness of factor analysis decomposition

An important question to consider is the reliability of our factor analysis. We have explored this in depth, by 1) comparing with the only real alternative, what we call a flat average weighting of dimensions, based upon intuition, and 2) a bootstrapping procedure to determine whether there is substantially more uncertainty associated with the loadings arising from the factor analysis than from the flat average. On the basis of these two explorations, we do not see evidence for substantial unreliability arising from the factor analysis. These explorations can be found in Appendix A4 (titled "Justification of factor analysis decomposition").

Additionally, the factor loadings we obtain are actually very intuitive and what one would expect if they were placed just on the basis of the expected influence of different variables. To see this, consider Figure A4.2 in the Appendix/supplementary material, which gives the factor loadings across the seven underlying variables. As justified in Appendix 4 (subsections "Background to Analysis" and "Comparison to Flat Average"), the key question that the factor analysis answered was where should the Aura variable end up – with Headache or Visual Stress? The factor analysis indicated that on the basis of the data collected, it is more appropriately placed with Visual Stress.

4.8. Potential limitations

There are a few limitations to the reported work. As the replies to the questionnaires, as well as the discomfort ratings during the experiment, are self-reported, there is subjectivity in the derived factors, for example, headache regularity. Enlarging the data set and collecting headache diaries would increase the reliability of our findings.

As discussed in the methods, our factor analysis produced three factors: visual stress, headache and discomfort. As already stressed, there is collinearity between the regressors that result from combining the factor scores and change through time (i.e. partitions or onsets). To ensure that no effect in the data is accounted for twice, the headache-time change interaction and discomfort-time change interaction regressors were also orthogonalized with respect to the visual stress-time change interaction regressor and then with respect to each other. This choice is justified as visual stress was the strongest factor obtained from the factor analysis and consequently, the other two factors were orthogonalized with respect to it. The findings with these orthogonalized regressors are presented in supplementary material/appendix A5. This issue deems our non-orthogonalized findings as exploratory, with our most robust findings being those that came out both non-orthogonalized and orthogonalized; see Table 8.

A number of commentators have rightly highlighted the problem of partial presentation of analyses performed (Bishop, 2020). If many contrasts are tested within an experimental or analysis trajectory, but the results of only a few contrasts, typically those that came out significant, are reported, then it is difficult for the reader to assess the vulnerability to false positives. Accordingly, we want the reader to recognise that the results presented in this paper were part of an analysis trajectory that includes results presented in a companion paper (Dogan et al., 2025), and in both this paper and (Dogan et al., 2025), we have presented a table summarising all the contrasts run; see Table 8 in this paper and table 11 in (Dogan et al., 2025). Importantly, the general pattern in both papers is to observe habituation (but not sensitization) across partitions and sensitization (but not habituation) across onsets, with these temporal patterns increasing with clinical condition (i.e., as one moves up factors).

Overall, though, given the novelty of the effects identified, all our interactions need to be replicated before they can be considered robust findings.

Importantly, the time-series and line-chart visualisations that we give for our statistical findings (such as, the visualisation in panel 14(b) of the statistical effects in panel 14(a)) are a good, but not a perfect

representation of the statistical finding. This is because the median split we perform on the Headache factor, which is required for the visualisation, does not perfectly reflect the factor score continuous regressor. For example, all those high on the headache factor contribute identically to the median split, but the continuous regressor weights those in the high group with higher scores more than those with smaller scores.

In addition to the inherent subjectivity of self-reported measures, the retrospective nature of our headache assessment may introduce recall bias. Unlike prospective headache diaries typically used in clinical settings to monitor migraine and headache symptoms, our questionnaire relied on participants' recollections over the past three months. This reliance on memory may affect the accuracy of measures such as headache frequency, duration, intensity, and aura—factors that are critical to constructing the Headache factor. Although our questionnaire is based on validated measures and has been widely used in headache research, future studies would benefit from incorporating prospective tracking methods (e.g., headache diaries) to enhance the reliability and precision of these estimates.

From a methodological perspective, it is also important to realise that difficulties in accurately recalling headache characteristics would add noise in our data. This would in turn reduce statistical power and thus, lead to type-II errors. It is possible, but much less likely that this noise would "lineup" consistently across individuals and increase the false-positive rate. So, in other words, difficulties in accurately remembering are much more likely to reduce the size of our effects, than spuriously increase them. This would lead to us underestimating our effects, i.e. leading to type-II errors, rather than type-I errors.

A potential confound for our findings is that the 3c/deg medium frequency stripes are close to the peak of the visual contrast sensitivity function and thus may exhibit an enhanced response for that reason. In other words, the extreme effects we observe on our Pattern-Glare Index (PGI) may simply reflect an increased electrical brain response to high contrast stimuli. However, importantly, we do exhibit effects on our pattern-glare index that vary systematically with our headache factor, e.g. PGI increasing as one progresses up the headache factor. For such an effect to be explained by contrast sensitivity, one would require those susceptible to headaches to exhibit an increased contrast sensitivity. However, there is little evidence for such an increase. In fact, some have seen the reverse; for example, McKendrick and Sampson (2009) suggested that migraineurs exhibit reduced visual contrast sensitivity for visual gratings at the frequency of our Medium stimulus. Although, it is possibly that there is no difference in contrast sensitivity for migraineurs (Asher, O'Hare and Hibbard, 2021). These failures to find an increased contrast sensitivity makes it unlikely that what we have interpreted as increases in hyper-excitation in the brain, could be explained away as simple changes in brain response due to changes in contrast sensitivity.

4.9. Future research

Increasing the size of the dataset would enable us to investigate quartiles of participants, rather than just median splits. The analyses could then directly contrast and visualise participants who have scored the highest on a factor and those who have scored the lowest. This would enable us to characterize more targeted population groups.

Furthermore, as our participants belonged to a healthy group, another exciting research direction is to perform the same analyses for migraine/headache sufferers. This would offer the opportunity to relate the findings to previous research and to investigate whether the effects we have seen for a healthy group carry over to a clinically relevant group. In this way, these electrophysiological findings could potentially provide a biomarker to help in migraine diagnosis.

5. Conclusion

Ultimately, we have provided evidence that hyperexcitability in the visual cortex during the pattern-glare test exists in the healthy population and manifests as an increased overall amplitude for the aggravating (Medium) stimulus. Sensitization to the aggravating medium spatial-frequency stimulus was identified over a short time-frame, while habituation to the same stimulus was identified over a longer time-frame. Both this sensitization and habituation was dependent on susceptibility to headaches.

Notably, we have found similar effects, sensitization through onsets and habituation through partitions, for another part of our experimental paradigm. The current paper focussed on the evoked transients following stimulus onset. However, we have also analysed the electrical response in the longer (3 s) period while the stimulus is on and continuously driving the participants' brain. In many respects, the findings in this sustained period of stimulation (Jefferis et al., 2024) are more easily interpreted and more compelling than those presented here on the onset transients.

These results suggest that this same experimental paradigm and analysis should be performed on a clinically diagnosed population.

CRediT authorship contribution statement

Cihan Dogan: Writing – review & editing, Writing – original draft, Visualization, Validation, Software, Methodology, Investigation, Formal analysis. **Claire E. Miller:** Writing – review & editing, Validation, Supervision, Resources, Project administration, Methodology, Investigation, Funding acquisition, Formal analysis, Data curation, Conceptualization. **Tom Jefferis:** Writing – review & editing, Validation, Software, Methodology, Investigation. **Margarita Saranti:** Writing – review & editing. **Austyn J. Tempesta:** Writing – review & editing, Visualization, Software, Resources, Project administration, Investigation, Funding acquisition, Formal analysis, Data curation, Conceptualization. **Andrew J. Schofield:** Writing – review & editing, Visualization, Validation, Supervision, Resources, Project administration, Methodology, Investigation, Funding acquisition, Formal analysis, Data curation, Conceptualization. **Ramaswamy Palaniappan:** Writing – review & editing, Validation, Supervision, Software, Investigation. **Howard Bowman:** Writing – review & editing, Writing – original draft, Visualization, Validation, Supervision, Software, Resources, Project administration, Methodology, Investigation, Funding acquisition, Formal analysis, Data curation, Conceptualization.

Declaration of competing interest

The authors report no competing interests.

Appendix A. Supplementary data

Supplementary data to this article can be found online at https://doi.org/10.1016/j.ynirp.2025.100271.

Data availability

Data will be made available on request.

References

Adjamian, P., Holliday, I.E., Barnes, G.R., Hillebrand, A., Hadjipapas, A., Singh, K.D., 2004. Induced visual illusions and gamma oscillations in human primary visual cortex. Eur. J. Neurosci. 587–592.
Arfken, G., 1985. Gram-schmidt orthogonalization. Mathematical Methods for Physicists, pp. 516–520.
Asher, J.M., 2021. No evidence of reduced contrast sensitivity in migraine-with-aura for large, narrowband. Centrally Presented Noise-Masked Stimuli. MDPI, Basel.
Bishop, D., 2020. How scientists can stop fooling themselves over statistics. Nature.
Bowman, H., Brooks, J.L., Hajilou, O., Zoumpoulaki, A., Litvak, V., 2020. Breaking the circularity in circular analyses: simulations and formal treatment of the flattened average approach. PLoS Comput. Biol.
Brainard, D.H., 1997. The Psychophysics Toolbox, pp. 433–436.

Braithwaite, J.J., Marchant, R., Takahashi, C., Dewe, H., Watson, D.G., 2015. The Cortical Hyperexcitability Index (CHi): a new measure for quantifying correlates of visually driven cortical hyperexcitability. Cognitive Neuropsychiatry, pp. 330–348.
Braitwaite, J., Broglia, E., Bagshaw, A., Wilkins, A., 2013. Evidence for elevated cortical hyperexcitability and its association with out-of-body experiences in the non-clinical population: new findings from a pattern-glare task. Cortex 793–805.
Brazzo, D., Di Lorenzo, G., Bill, P., Fasce, M., Papalia, G., Veggiotti, P., Seri, S., 2011. Abnormal visual habituation in pediatric photosensitive epilepsy. Clin. Neurophysiol. 16–20.
Brooks, J.L., Zoumpoulaki, A., Bowman, H., 2017. Data-driven region-of-interest selection without inflating Type I error rate. Psychophysiology 100–113.
Conlon, E.G., Lovegrove, W.J., Chekalu, E., Pattison, P.E., 1999. Measuring visual discomfort. Vis. Cogn. 637–663.
Conlon, E., Lovegrove, W., Barker, S., Chekaluk, E., 2001. Visual discomfort: the influence of spatial frequency. Perception.
Coppola, G., Pierelli, F., Schoenen, J., 2009. Habituation and migraine. Neurobiol. Learn. Mem. 249–259.
Dogan, C., Jefferis, T., Saranti, M., Tempesta, A., Miller, C., Schofield, A., Bowman, H., 2025. Discomfort and Visual Stress Hyperexcitation Sensitises and Habituates on Different Time Scales: an Event Related Potential Study of Pattern-Glare. preparation.
Evans Bj, S.S., 2008. The Pattern Glare Test: a review and determination of normative values. Ophthalmic Physiol. Opt. 295–309.
Flandin, G., Friston, K.J., 2017. Analysis of family-wise error rates in statistical parametric mapping using random field theory. Hum. Brain Mapp.
Fong, C.Y., Law, W.H., Braithwaite, J., Mazaheri, A., 2020. Differences in early and late pattern-onset visual-evoked potentials between self- reported migraineurs and controls. Neuroimage Clinical.
Gerber, W.D., Kropp, P., 1995. Contingent negative variation during migraine attack and interval: evidence for normalization of slow cortical potentials during the attack. Cephallalgia.
Haigh, S.M., Chamanzar, A.M., Grover, P., Behrmann, M., 2019. Cortical hyper-excitability in migraine in response to chromatic patterns. The Journal of Head and Face Pain.
IHS, 2018. The International Classification of Headache Disorders, third ed. International Headache Society (IHS).
Jefferis, T., Dogan, C., Miller, C.E., Karathanou, M., Tempesta, A., Scofield, A.J., Bowman, H., 2024. Sensitization and habituation of hyper-excitation to constant presentation of pattern-glare stimuli. Neurol. Int. 1585–1610.
Khalil, N., 2000. Long term decline of P100 amplitude in migraine with aura. J. Neurol. 507–511.
Kleiner, M., Brainard, D., Pelli, D., Ingling, A., Murray, R., Broussard, C., 2007. What's new in Psychtoolbox-3. Perception 1–16.
McKendrick, A.M., 2009. Low Spatial Frequency Contrast Sensitivity Deficits in Migraine Are Not Visual Pathway Selective. SAGE Publications, London.
Mickleborough, M.J., Chapman, C.M., Toma, A.S., Chan, J.H., Truong, G., Handy, T.C., 2014. Interictal neurocognitive processing of visual stimuli in migraine: evidence from event-related potentials. PLoS One.
Nulty, D.D., Wilkins, A.J., Williams, M.G., 1987. Mood, pattern sensitivity and headache: a longitudinal study. Psychol. Med. 705–713.
Obrig, H., Israel, H., Kohl-Bareis, M., Uludag, K., Wenzel, R., Müller, B., Villringer, A., 2002. Habituation of the visually evoked potential and its vascular response: implications for neurovascular coupling in the healthy adult. Neuroimage 1–18.
Oelkers, R., Grosser, K., Lang, E., Geisslinger, G., Kobal, G., Brune, K., Lotsch, J., 1999. Visual evoked potentials in migraine patients: alterations depend on pattern spatial frequency. Brain 1147–1155.
Omland, P.M., Uglem, M., Hagen, K., Linde, M., Tronvik, E., 2016. Visual evoked potentials in migraine: is the "neurophysiological hallmark" concept still valid? Clin. Neurophysiol. 810–816.
Oostenveld, R., Fries, P., Maris, E., Schoffelen, J., 2011. ieldTrip: open source software for advanced analysis of MEG, EEG, and invasive electrophysiological data. Comput. Intell. Neurosci.
Pelli, D.G., 1997. The VideoToolbox software for visual psychophysics: transforming numbers into movies.Pelli, D. G. Spat. Vis. 437–442.
Schoenen, J., Wang, W., Albert, A., Delwaide, P.J., 1995. Potentiation instead of habituation characterizes visual evoked potentials in migraine patients between attacks. Eur. J. Neurosci. 115–122.
Tempesta, A.J., Miller, C.E., Litvak, V., Bowman, H., Schofield, A.J., 2021. The missing N1 or jittered P2: electrophysiological correlates of pattern glare in the time and frequency domain. Eur. J. Neurosci.
Trappenberg, T.P., 2009. Fundamentals of Computational Neuroscience.
Welch, K.M., D'Andrea, G., Tepley, N., Barkley, G., Ramadan, N.M., 1990. The concept of migraine as a state of central neuronal hyperexcitability. Neurological Clinics 817–828.
Wilkins, A., 1986. Intermittent illumination from visual display. Hum. Factors.
Wilkins, A.J., 2015. A physiological basis for visual discomfort: application in lighting design. Light. Res. Technol.
Wilkins, A.J., Evans, B.J., 2001. Pattern Glare Test Instructions. IOO Sales Ltd, London, UK.
Wilkins, A., Nimmo-Smith, I., Tait, A., McManus, C., Sala, S.D., Tilley, A., Scott, S., 1984. A neurological basis for visual discomfort. Brain 989–1017.